THE JOURNAL OF COMPARATIVE NEUROLOGY 301:461–489 (1990)

The Dopaminergic Amacrine Cell

DENNIS M. DACEY
Department of Biological Structure, The University of Washington,
Seattle, Washington, 98195

ABSTRACT

The detailed morphology of the dopaminergic amacrine cell type has been characterized in the macaque monkey retina by intracellular injection of horseradish peroxidase (HRP). This cell type was recognized by its large soma in an in vitro, wholemount preparation of the retina stained with the fluorescent dye, acridine orange. HRP-fills revealed a large, sparsely branching, spiny dendritic tree and a number of extremely thin, axon-like processes that arose from the soma and proximal dendrites. The axon-like processes were studded with distinct varicosities and were traced for up to 3 mm beyond the dendritic tree. The true lengths of the axon-like processes were greater than 3 mm, however, because the HRP reaction product consistently diminished before an endpoint was reached. Both the dendrites and the axon-like processes were narrowly stratified close to the outer border of the inner plexiform layer, although in a few cases single axon-like processes projected into the outer nuclear and outer plexiform layers.

The HRP-filled amacrines appeared equivalent to a subpopulation of neurons that are intensely immunoreactive for tyrosine hydroxylase (TH). TH-immunoreactive cells showed a nearly identical soma size and dendritic field size range, the same pattern of dendritic branching and spiny morphology, and also gave rise to distinct axon-like processes from both the soma and proximal dendrites.

To test this correspondence more directly, the large acridine stained cells were injected with Lucifer Yellow and the retina was subsequently processed for TH immunoreactivity using diaminobenzidine as the chromagen. In all cases Lucifer Yellow injected cells also showed intense TH immunoreactivity.

Spatial densities of the TH amacrine cells were therefore used to calculate coverage factors for the dendritic trees and for the axon-like components of the HRP-filled cells. The axon-like processes showed a coverage factor of at least 300, about 100 times that of the dendritic fields. This great overlap could be directly observed in TH-immunoreacted retinal wholemounts as a dense plexus of fine, varicose processes. The density of the TH plexus is greater than the density predicted from the lengths (1–3 mm) of the HRP-filled axon-like processes however, and suggests that the axon-like processes have an actual length of about 4–5 mm.

The dual morphology of the dopaminergic amacrine, coupled with the previous studies of identified dopaminergic synapses, suggests the hypothesis that the varicosities on the axon-like processes are the major source of synaptic output, and that the spiny dendrites are the major recipients of synaptic input from cone bipolar cells and other amacrine cells.

The rare extension of the axon-like processes into the outer plexiform layer, and current understanding of the morphology of dopaminergic interplexiform cells in teleost fish, supports the hypothesis that the dopaminergic amacrine and interplexiform cells represent a single cell type in which there is quantitative variation across species in the projection pattern of the axon-like processes.

Key words: retina, primate, in vitro, horseradish peroxidase, tyrosine hydroxylase

The mammalian retina contains a subpopulation of dopaminergic amacrine cells whose distinctive morphology suggests a significant role for the release of dopamine in the passage of rod signals to ganglion cells. As revealed by catecholamine histofluorescence or with antisera to tyrosine hydroxylase, the dopaminergic amacrine cells display large, sparsely branched dendritic trees narrowly stratified near the scleral border of the inner plexiform layer (Brecha et al., '84; Mariani and Hokoc, '88; Nguyen-Legros, '88;

Accepted July 20, 1990.

Oyster et al., '85; Törk and Stone, '79; Versaux-Botteri et al., '86). These dendrites are embedded in a dense plexus of fine, varicose processes. Some of these processes form numerous ringlike structures that lie in a regular array throughout the plexus. In the cat's retina many, if not all, of the varicose rings encircle, and are presynaptic to, the somata of another identified amacrine cell type, the AII amacrine (Pourcho, '82; Voigt and Wässle, '87), and the distribution of rings appears to reflect the distribution of AII somata (Vaney, '85). In both cat and rabbit retina the AII amacrine also receives synaptic input from rod bipolar cells and is presynaptic to cone bipolar cells and ganglion cells (Famiglietti and Kolb, '75; Sterling, '83; Strettoi et al., '89), thus providing a synaptic pathway for the transmission of rod signals to ganglion cells. The synaptic contacts made by the dopaminergic cell onto the AII cell are therefore clearly implicated in the control of signal transmission through the rod pathway. This idea is consistent with the general finding that application of dopamine and its antagonists alters the sensitivity, but not the spatial structure, of ganglion cell receptive fields (Jensen and Daw, '84, '86; Thier and Alder, '84).

A more precise understanding of the role of the dopaminergic amacrine cell in the visual process has been difficult to achieve. One problem is that the complete and characteristic morphology of a single dopaminergic amacrine cell has not been determined. This is a significant gap because the way in which the varicose plexus, apparently a major source of dopaminergic synapses, is linked to the dendritic tree of an individual dopaminergic cell is not readily apparent from tyrosine hydroxylase immunoreactivity. A cone bipolar input to the dendritic tree of the dopaminergic cell has recently been identified (Hokoc and Mariani, '87, '88). However, it is not clear how this cone bipolar input is spatially related to the synaptic output to the AII amacrine cell. To address this question the detailed morphology of a single cell must be established and the synaptic organization of identified parts of the cell subsequently determined.

A picture of the complete morphology of the dopaminergic cell would also help to clarify the relation between the dopaminergic amacrine and interplexiform cells in the mammalian retina. It is not yet clear whether they represent two distinct cell populations which may coexist in the same retina (Oyster et al., '85) or represent variation across species or even variation within a single retina in the laminar distribution of processes of a single dopaminergic cell type (Wässle and Chun, '88).

Intracellular injections of Lucifer Yellow in formaldehyde fixed tissue have recently been used in rabbit (Tauchi and Masland, '88) and cat retina (Voigt and Wässle, '87) to determine the morphology of amacrine cells identified by catecholamine histofluorescence. Lucifer Yellow-filled cells in these studies displayed the same basic pattern of dendritic morphology that is apparent in tyrosine hydroxylase immunoreacted retinas. However, the origin of the varicose plexus and its rings was not apparent, perhaps because of the difficulty of observing extremely thin processes with Lucifer Yellow-fills in fixed tissue. Another approach was taken by using intracellular HRP injections in a living, in vitro preparation of the retina (Dacey, '86, '88). Potential dopaminergic amacrine cells were identified by a novel in vitro fluorescence that was induced by uptake of dopamine and the indolaminergic transmitter analogue 5,7-dihydoxytryptamine (5,7-DHT). The HRP-filled amacrine cells were characterized by extremely long and thin varicose processes that arose abruptly from the distal tips of the thick primary dendrites and extended for ~3 mm beyond the dendritic tree. It was suggested that the great overlap of these axon-like processes could account for the varicose plexus, and that the varicose rings would therefore be formed by the convergence of processes arising from many different cells spread widely over the retina. A major problem with this result is that there is no direct evidence that the cells identified after monoamine uptake are actually equivalent to the large dopaminergic cells previously identified by tyrosine hydroxylase immunoreactivity.

This study has taken another approach to characterizing the morphology of the dopaminergic amacrine cells. The vital fluorescent marker acridine orange was used to nonselectively label neurons in an in vitro preparation of the macaque monkey retina (Tauchi and Masland, '85). Under certain conditions a subpopulation of amacrine cells with large somata fluoresced more brightly than their neighbors. Intracellular injection of HRP or Lucifer Yellow into these cells revealed a morphologically distinct amacrine cell subpopulation. The soma size, depth of stratification, and primary dendritic branching pattern of the injected cells appeared identical to the large, intensely stained tyrosine hydroxylase immunoreactive cells of the macaque retina. Subsequent identification of Lucifer Yellow-filled cells as tyrosine hydroxylase immunoreactive by double labeling confirmed that the large, acridine stained amacrine cells were equivalent to the dopaminergic amacrine cells.

A striking feature of the HRP-filled dopaminergic amacrine cells is the presence of multiple, axon-like processes that originate directly from the soma and from proximal dendrites and extend far beyond the dendritic tree. The axon-like processes thus appear to correspond to the fine, varicose processes of the dopaminergic plexus as suggested in the preceeding paragraph. However, comparison of the macaque dopaminergic amacrine with the monoamine-accumulating amacrine identified in the cat's retina (Dacey, '88) reveals two morphologically distinct cell types that share only the interesting property of bearing axon-like processes.

MATERIALS AND METHODS

This study is based on data from *Macaca nemestrina* (n = 22), *M. fascicularis* (n = 2), and *M. mulatta* retinas (n = 4) obtained from the Tissue Program of the Regional Primate Research Center at the University of Washington. The data from the three species appeared indistinguishable and are combined in the Results. Procedures for retinal dissection, in vitro maintenance of the retina, intracellular injection of HRP and Lucifer Yellow, and overall data analysis have also been given in a previous report concerning the morphology of another amacrine cell type in the macaque retina (Dacey, '89a). Many of the methods have been modified for the present study and for ease of reference these methods are repeated here in their entirety.

In vitro preparation

Eyes were removed from animals under deep barbiturate anesthesia. The anterior portion of the eye was cut away just posterior to the lens and the vitreous was removed from the remaining eyecup. The eyecup was then placed in oxygenated Ames medium (Ames and Nesbett, '81), and the retina was dissected. When the retina was freed from the sclera and choroid it was placed in Ames medium contain-

ing collagenase (~1 mg/ml, Type II, Sigma) for 30 seconds to 1 minute. By treating the retina briefly with collagenase in this way it was possible to remove any remaining vitreous that adhered to the retinal surface. Heated, 30% gelatin was poured onto the bottom of a superfusion chamber and formed a thin, transparent layer that became sticky to the touch as it congealed at room temperature. A series of radial cuts were then made in the retina and it was laid flat, vitreal side up in the chamber and was held in place by adhering to the tacky gelatin layer. The retina was viewed with either transmitted or episcopic illumination and retinal neurons were stained in vitro by adding a few drops of acridine orange (~1 mM solution in Ames medium) to the superfusate as it passed through the chamber. Additional acridine was added to the chamber at ~30 minute intervals throughout the experiment. The retina was maintained in vitro for several hours at room temperature by continuous superfusion (~3 ml/minute) with no apparent deterioration in cellular morphology at the light microscopic level.

Intracellular injections of HRP and Lucifer Yellow

Intracellular microelectrodes were formed from thin-walled microcapillary glass pulled to an initial resistance of 175–250 MΩ on a Brown-Flaming micropipette puller. The electrodes were filled with a 4% solution of rhodamine-conjugated HRP (Sigma) and Lucifer Yellow (Aldrich) in MOPS buffer (pH 7.6) and beveled to a final resistance of 30–40 MΩ with a K.T. Brown beveler. The epifluorescence microscope used to observe the in vitro fluorescence is equipped with a stage mounted micromanipulator such that microelectrodes can be positioned independently of focus (stage height). An oil-driven microdrive mounted to the manipulator was used to advance the microelectrode manually. The electrode tip and the retina were viewed together at high resolution with a 40× water-immersion, long working distance objective (Zeiss) that was modified to permit the proper angle of electrode approach to the tissue (Brown and Flaming, '86).

Both Lucifer Yellow (LY) fluorescence in the microcapillary electrode and the acridine fluorescence were observed with the same filter combination (excitation filter, 410–490 nm; barrier filter, 515 nm). This permitted the electrode tip to be positioned near a fluorescing cell under direct microscopic control. Cell penetration was achieved by tapping the base of the microscope and subsequently confirmed by iontophoresis of LY into the cell (0.1–1.0 nA, negative current for 5–10 seconds). If the penetration was successful the cell was then injected with rhodamine-HRP (3–8 nA, positive current; 1–3 minutes). The accumulation of rhodamine-HRP in the cell's dendritic tree and the quality of its morphology was directly monitored by observing an increase in rhodamine fluorescence (excitation filter, 545 nm; barrier filter, 590 nm) within the cell's processes during the course of the injection. Retinas were removed from the superfusion chamber after 6–8 hours and fixed in phosphate buffered 4% paraformaldehyde and 1% glutaraldehyde (0.1 M; pH 7.4) for 1–2 hours. HRP reaction product was demonstrated in the intact retinal wholemount using diaminobenzidine (DAB) as the chromagen (Dacey, '85). The retinas were mounted on a slide vitreal side up, dehydrated, cleared, and coverslipped without counterstaining.

Tyrosine hydroxylase immunohistochemistry

Immunoreactivity for tyrosine hydroxylase was demonstrated in *M. nemestrina* (n = 8) and *M. mulatta* (n = 2) retinas with a commercially available polyclonal antibody (Pel Freez) using the avidin-biotin complex (ABC) method. Retinas were dissected in oxygenated Ames medium and immersion fixed in 4% paraformaldehyde for 2 hours followed by a buffer rinse to remove excess fixative from the tissue. A series of radial cuts were made around the periphery of the retina to permit its later flatmounting on a slide. It was incubated in primary antisera at 5°C for 48 hours at a 1:100 dilution in Tris buffered saline (TBS) containing 0.2% Triton and 1% normal goat serum. After rinsing in TBS, retinas were incubated in biotinylated anti-rabbit IgG (1:100 dilution) for 45 minutes at 37°C. This antibody complex was then linked to avidin conjugated HRP by incubating the retinas in the Vectastain ABC solution (Vector Labs) for 45 minutes at room temperature. The HRP reaction product was subsequently demonstrated using diaminobenzidine (DAB) as the chromagen by preincubating retinas for 15 minutes in a 0.05% DAB solution followed by a final incubation in the same solution with 0.01% H_2O_2 added. The retinas were then rinsed in buffer and mounted flat, vitreal side up on a slide, dehydrated in alcohol, cleared in xylene, and coverslipped.

Topography of TH-immunoreactive cells

Several subpopulations of TH-immunoreactive cells were observed in all stained retinas. They could be distinguished by staining intensity, soma size, and dendritic stratification in the IPL. One population could be clearly distinguished by its large soma size, intense staining, and dendritic stratification near the scleral border of the IPL. These cells are the focus of the present study and will be referred to as the large, intensely staining TH amacrines. They correspond to the large, sparsely branching amacrine cells that have been observed previously in the primate retina by both catecholamine histofluorescence and tyrosine hydroxylase immunoreactivity (Mariani et al., '84; Nguyen-Legros et al., '84), and which have recently been distinguished from some of the other, less well characterized TH-positive cell types (Nguyen-Legros, '88; Mariani and Hokoc, '88). The spatial density of the large, intensely staining subpopulation was determined for the entire retina in a single *M. mulatta* retina by the following sampling scheme. Cells were counted in a 1 mm^2 field that was observed through a drawing tube at a total magnification of 125×. A total of 124 fields were sampled. Field centers were spaced 2 mm apart at eccentricities greater than 4 mm (47 fields total) where cell density did not change greatly as a function of eccentricity. Within 4 mm of the fovea the entire retina was sampled (77 fields total). Isodensity lines were interpolated by eye from the cell densities that were plotted on a tracing of the whole-mounted retina.

Lucifer Yellow-tyrosine hydroxylase double labeling

To determine whether the amacrine cells that were observed in vitro and injected with HRP corresponded to the large TH-positive cells, a sample of the large acridine stained cells was injected with just LY and subsequently processed for TH immunoreactivity. For these double labeling experiments the characteristic morphology of these cells was confirmed by direct microscopic inspection of the

LY-filled cell during the injection period. Pieces of retina containing the injected cells were then fixed by immersion in 4% paraformaldehyde for 2 hours and subsequently processed for tyrosine hydroxylase immunoreactivity. The ABC method was used according to the procedure described above for TH immunoreactivity; the antibody complex was demonstrated with HRP and DAB as the chromagen. Because the HRP reaction reduced the LY fluorescence significantly, the presence of both LY and TH immunoreactivity was documented sequentially rather than simultaneously. LY injected cells were located and photographed prior to performing the HRP reaction. After the HRP reaction the same cells were rephotographed. The TH-immunoreactive cells usually showed intense staining of the dendritic tree. In double labeled cases it was thus possible to clearly distinguish the same dendritic structure in both the LY photographs and after HRP staining. The double labeling could thus be confirmed not only in the cell body but also in the dendritic tree, which permitted verification of the characteristic stratification pattern of these cells at the outer border of the IPL.

Data analysis

Soma and dendritic field sizes were determined for a sample of 118 HRP-filled cells that appeared to be well filled. The reaction product within these cells appeared uniformly dark out to the distal dendritic tips. Cells judged to be incompletely filled showed lighter and non-uniform filling marked by gradual fading of the HRP reaction product in the distal dendrites. Soma area was determined by entering the soma outline (at 1,500×) into a computer via a graphics tablet. Soma diameter was expressed as the diameter of a circle with the same area. To calculate dendritic field area a convex polygon was traced around the dendritic field perimeter (at 400×) and entered into the computer. Dendritic field diameter was expressed as the diameter of a circle with the same area as that of the polygon.

For 103 injected cells the depths of stratification of the dendritic tree and soma within the IPL were determined from the wholemounts by reading the scale on the microscope focus knob (calibrated to 1 μm intervals). For each cell a depth reading was taken for the borders of the inner nuclear and ganglion cell layers with the IPL. These borders were judged by closing down the microscope condenser diaphragm and bringing the unstained cell bodies at the borders of the two cellular layers into focus. Measurements of IPL thickness made in this way were consistently 11–13 μm (the same measurements made in vitro after acridine staining gave an IPL thickness of ~35 μm, indicating a shrinkage of ~70% after mounting and dehydration). The depths at which the soma and the dendritic branches and axon-like processes were located were measured and expressed as a percentage of the total thickness of the IPL. The stratification of the axonal and dendritic trees of two other cells was determined by making camera lucida tracings with a computer system (Eutectics) designed to preserve z-axis depth information, and using the computer to rotate the cells by 90°.

RESULTS

Identification of DA-like amacrine cells in vitro

Acridine orange revealed apparently all retinal neurons when applied to the in vitro preparation, but the intensity of the fluorescence in some cells varied under certain conditions. Figure 1 compares the pattern of acridine fluorescence in the ganglion cell and inner nuclear layers in peripheral retina. In the ganglion cell layer the fluorescence showed a pattern characteristic of basophilic dye stains like toluidine blue or cresyl violet: the perikarya and the nucleoli fluoresced intensely and the nuclei were unstained (Fig. 1A). By contrast, individual cell bodies were much more difficult to distinguish in the inner nuclear layer because most of the cells were smaller and more densely packed, and showed less cytoplasm. Some optical resolution also appeared to be lost when focusing through the ganglion cell layer. However, the quality of the acridine staining showed a characteristic change after the retina had been in

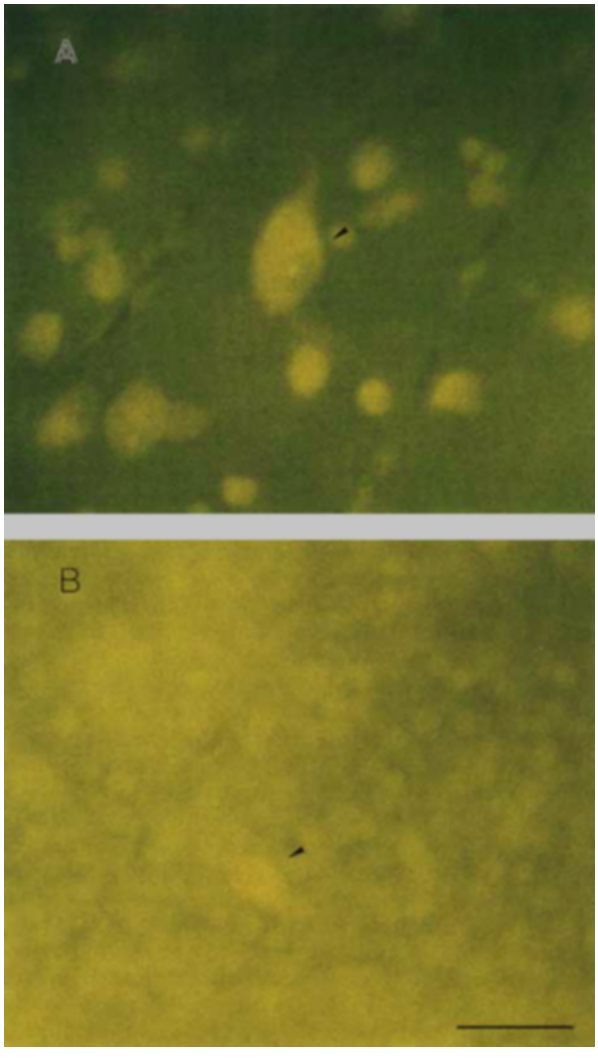

Fig. 1. Acridine orange fluorescence in a wholemount, in vitro preparation of *Macaca nemestrina* retina. **A:** Plane of focus is at the ganglion cell layer in the peripheral retina. Cells of different sizes and shapes accumulate the dye and fluoresce yellow-green under blue episcopic illumination. The soma of a large, parasol ganglion cell is indicated by the arrowhead. **B:** The plane of focus is shifted to the inner border of the inner nuclear layer and shows a densely packed array of smaller, more weakly fluorescent cells. A larger and more intensely fluorescent cell body (arrowhead), present at a much lower spatial density, was targeted for intracellular injection of HRP or Lucifer Yellow. Scale bar = 25 μm.

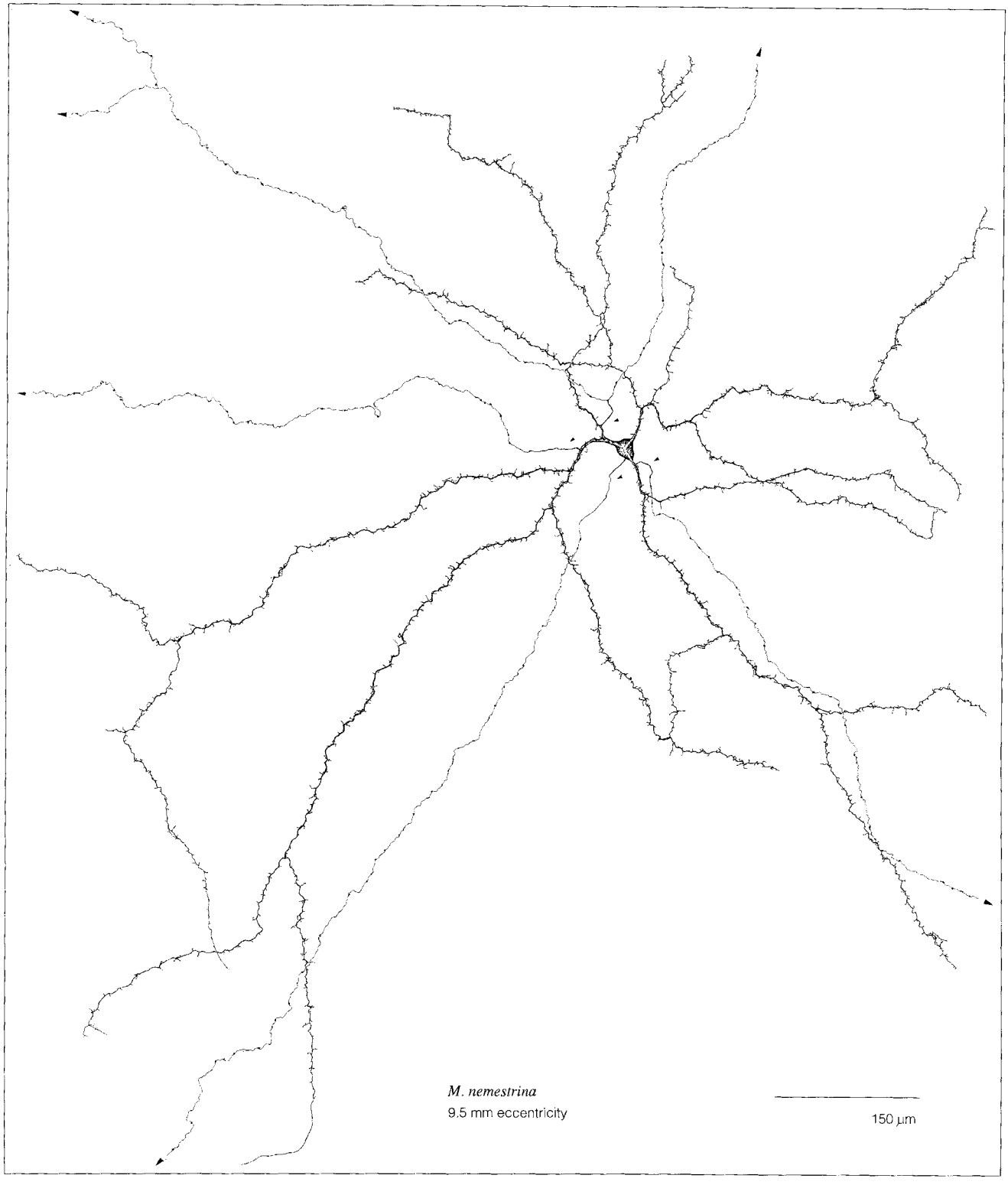

Fig. 2. Camera lucida tracing of the dendritic tree and the proximal axon-like processes of an HRP-filled DA-like amacrine cell. The dendrites are sparsely branching and give rise to a large number of complex spine-like appendages. Distinct axon-like processes originate from the soma and the thick proximal dendrites close to the soma (small arrowheads). They are thin and smooth but bear distinct varicosities. The axon-like processes branch only sparsely and radiate beyond the dendritic tree for 1–3 mm. (The large arrowheads indicate that the axon-like processes extend beyond the field shown.) The total size of dendritic tree and axon-like processes observable after intracellular HRP injection is illustrated at lower magnification in Figure 3.

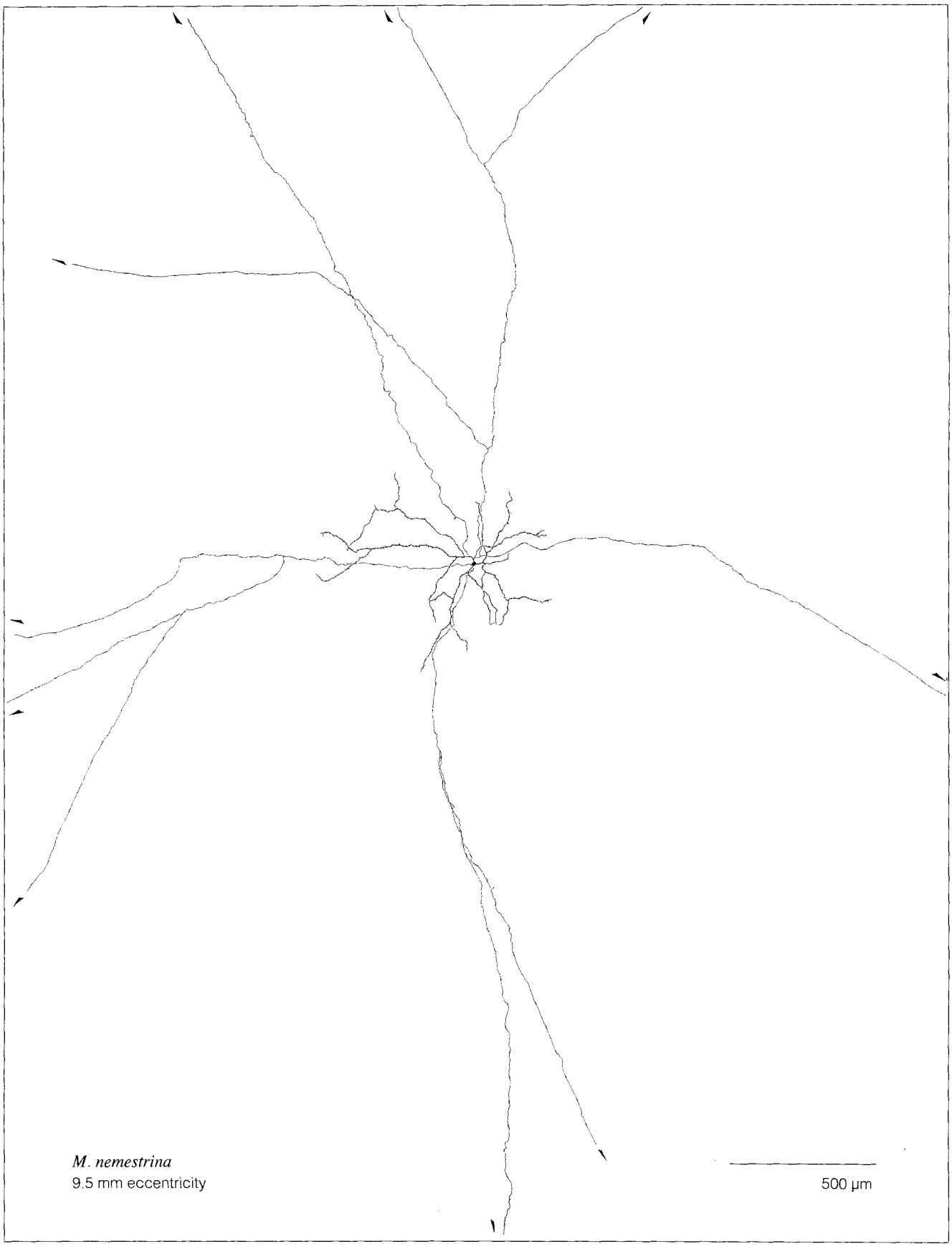

Figure 3

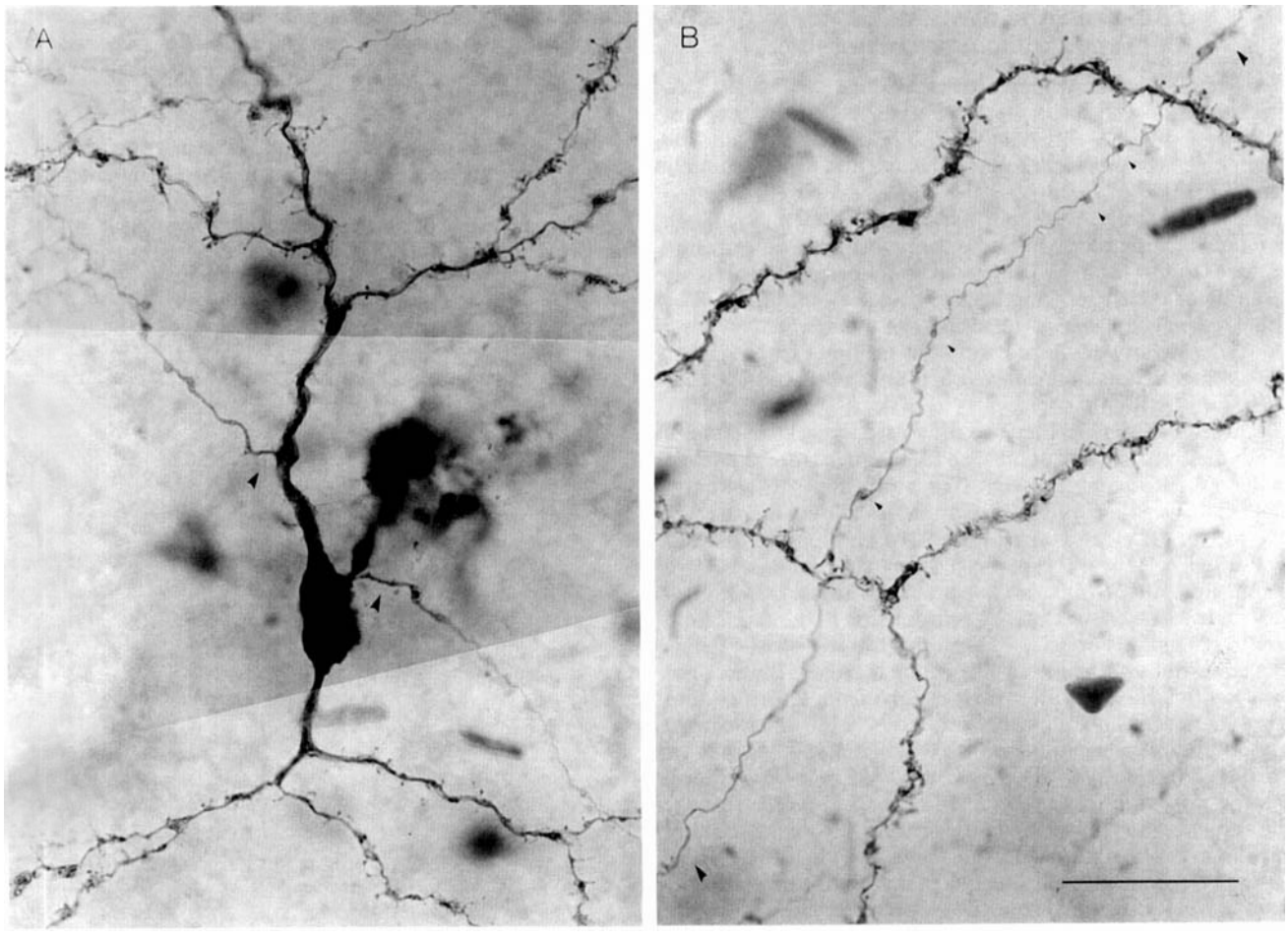

Fig. 4. Photomicrographs of an HRP-filled DA-like amacrine cell illustrates the distinct morphologies of the dendritic tree and the axon-like processes. **A:** Proximal dendritic tree and origin of axon like processes from the soma and a thick primary dendrite (arrowheads). Camera lucida tracings of this cell are illustrated in Figures 7 and 18B. **B:** distal dendrites and a single axon-like process (located between the large arrowheads). The dendrites are thick and covered with spines and the axon-like process is thin and smooth and bears large varicosities (some are indicated by the small arrowheads); both processes are narrowly stratified in the same plane, close to the outer border of the inner plexiform layer. Scale bar = 50 μm.

vitro for about 3–4 hours. Exposure to blue excitation for a few seconds induced a relatively intense fluorescence in a subset of large cells in the inner tier of cells in the inner nuclear layer (Fig. 1B). These cells appeared at a relatively low density (typically only one cell was observed in an exposed field about 200 μm in diameter), and showed a large multipolar or fusiform cell body ~ 15 μm in diameter. It was surprising that these large cells were not visible earlier in the experiment, but the time course of their appearance was remarkably consistent. This late appearing, distinctive fluorescence also occurred in certain other amacrine cell bodies, but they have yet to be studied systematically by intracellular injection. There is no clear explanation for this time course and pattern of fluorescence, but it seems plausible that some retinal cells accumulate greater amounts of acridine orange, that could, over a period of 3–4 hours, lead to a relatively stronger signal in these cells. Regardless of its mechanism, the more intense fluorescence in these distinctive, large cells allowed them to be selectively targeted for intracellular injection of HRP or Lucifer Yellow.

A total of 118 HRP-filled cells provided the database for this study; all the cells showed a characteristic soma size, morphology, and narrow depth of stratification near the outer border of the IPL. A striking feature of these amacrine cells was the presence of two distinct morphological components which will be referred to as the dendritic tree and the axon-like processes. Evidence will be presented in a subsequent section of the Results that these cells are equivalent to the large, intensely staining subpopulation of TH-immunoreactive cells. Until then these cells will be referred to as the DA-like amacrine cells.

Fig. 3. Complete camera lucida tracing of the HRP-filled DA-like amacrine cell illustrated in Figure 2. In this tracing the dendritic tree is at the center of the figure and the axon-like processes are the thin lines that radiate beyond the dendritic tree. At this magnification the varicosities along the axon like process could not be illustrated. The axon-like processes tend to follow a straight course and to branch once or twice. The arrowheads indicate that the axon-like processes did not appear to terminate but could not be traced further because the HRP reaction product gradually diminished.

The soma and the dendritic tree of the DA-like amacrine cells

A complete camera lucida tracing of an HRP-filled DA-like amacrine cell located in the nasal periphery 9.5 mm from the fovea is illustrated in Figures 2 and 3. The dendritic tree was sparsely branched and conspicuously spiny. Primary dendrites, ~1–2 μm in diameter, radiated in approximately the same plane as the cell body. Each dendrite bifurcated close to the soma and gave off only one or two more long branches that followed a relatively straight or gently curving course before terminating. The spines densely covered most of the dendritic tree and showed a variety of shapes and sizes, ranging from simple, thread-like extensions to branched and lobulated appendages (Fig. 4A,B).

The scatter plots in Figure 5 illustrate the relationship of dendritic tree size and soma size to distance from the fovea for the entire sample of DA-like amacrine cells. Ninety-eight cells were recovered from animals ranging in age from 2.5 to 16 years and are plotted in Figure 5A. Twenty well-filled cells were recovered from the retinas of two young juvenile *M. nemestrina* monkeys (ages 1.2 and 1.3 years). It was evident that the relationship of dendritic field size to retinal eccentricity was different in these two retinas and these data were plotted separately in Figure 5C. Retinal location for the HRP-filled cells ranged from 2.3 to 16 mm from the fovea. The majority of the cells (94%) were located in the retinal periphery at an eccentricity of 6 mm or greater. The sample was biased towards more peripheral cells because in central retina, from 0 to 3 mm eccentricity, the thickness of the optic fiber layer and the dense packing of cells in the ganglion cell layer made it difficult to clearly observe the acridine fluorescence in the inner nuclear layer. For the older retinas (Fig. 5A) dendritic field diameter ranged from 299 μm at 3.2 mm eccentricity to 734 μm in the retinal periphery (n = 98, mean ± SD = 510 ± 82 μm). The field size showed a small but significant positive correlation with distance from the fovea ($P < 0.01$). However, there appeared to be little influence of eccentricity on field size at eccentricities greater than 7–8 mm, and sizes were quite variable, ranging from ~400 μm to ~700 μm in diameter. By contrast, dendritic field size actually appeared to decrease in peripheral retina for the smaller sample of 20 cells recovered from young juvenile retinas. It is likely that the peripheral cells have not yet reached their adult size because there is evidence that the retinal periphery is still growing at this age (Packer et al., '90) and will increase in area by 30% between 1 and 5 years of age.

Soma diameter for the DA-like amacrine cells ranged from 11.2–16.6 μm (n = 112, mean ± SD = 13.5 ± 1.1). Soma diameter was only weakly correlated with distance from the fovea at the retinal eccentricities in this sample (Fig. 5B). There was a trend for smaller cell bodies at eccentricities of less than 4 mm, but, like dendritic field size, soma size was variable in the retinal periphery and there were not enough data points in central retina to make a clear comparison with the more peripheral sample.

Although dendritic trees tended to be larger for more peripheral cells they showed a similar dendritic branching pattern. A camera lucida tracing of the DA-like cell nearest to the fovea (Fig. 6, 2.6 mm eccentricity) is compared to a large cell from the retina periphery (Fig. 7, 8.8 mm eccentricity). Both cells clearly displayed the characteristic spiny and sparsely branched dendrites. Both cells showed 12 dendritic branchpoints so that the increase in dendritic field size for the larger cell appeared to be due to an increase in the length of the long, interbranchpoint segments with little change in the number of dendritic branches. This constancy in branchpoint number is further shown in the scatter plot in Figure 8 for a sample of 23 DA-like cells. The number of branchpoints ranged from 9 to 17 (mean ± SD = 12.6 ± 1.9) and was not influenced by retinal eccentricity. The narrow range of branchpoints suggests that it may be a size independent, and characteristic property of the DA-like cell type.

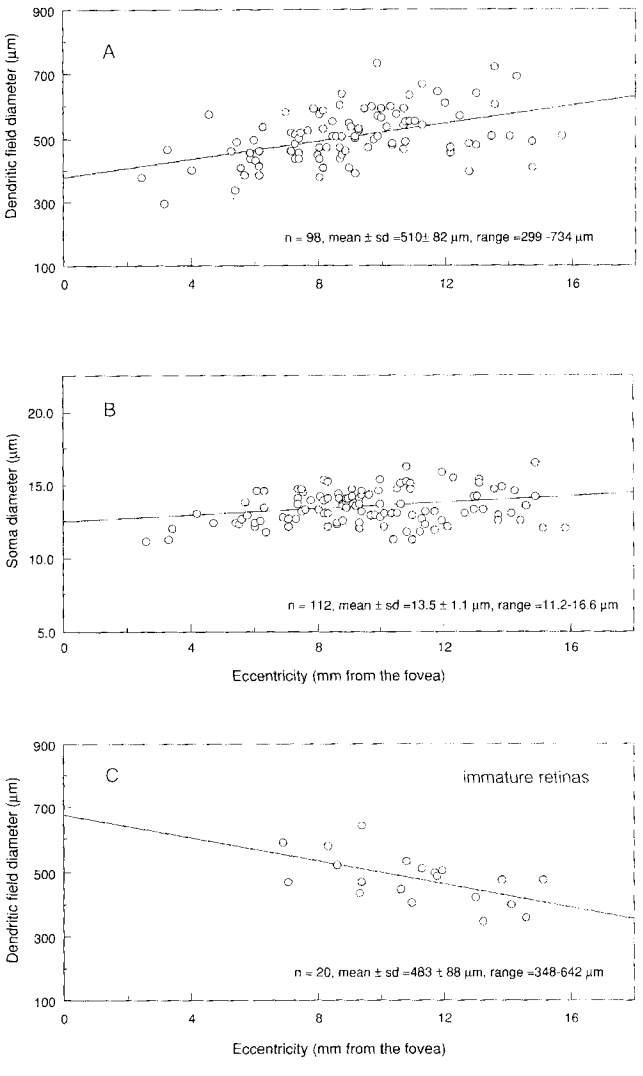

Fig. 5. Scatterplots of dendritic tree and soma size as a function of retinal eccentricity for the DA-like amacrine cells. **A:** A weak, but significant, positive correlation of dendritic field size with eccentricity was observed ($P < .01$). Because of the high density of cells and the reduction in soma size it was difficult to inject cells within 4 mm of fovea in acridine stained retinas. **B:** Soma size also showed a weak but significant positive correlation with eccentricity ($P < .02$). Soma size was not measured in 6 cells in the sample because HRP leakage around the cell body obscured its outline. **C:** In two retinas from animals aged 1.3 and 1.4 years dendritic field size actually decreased with increasing retinal eccentricity presumably because peripheral retina is still growing.

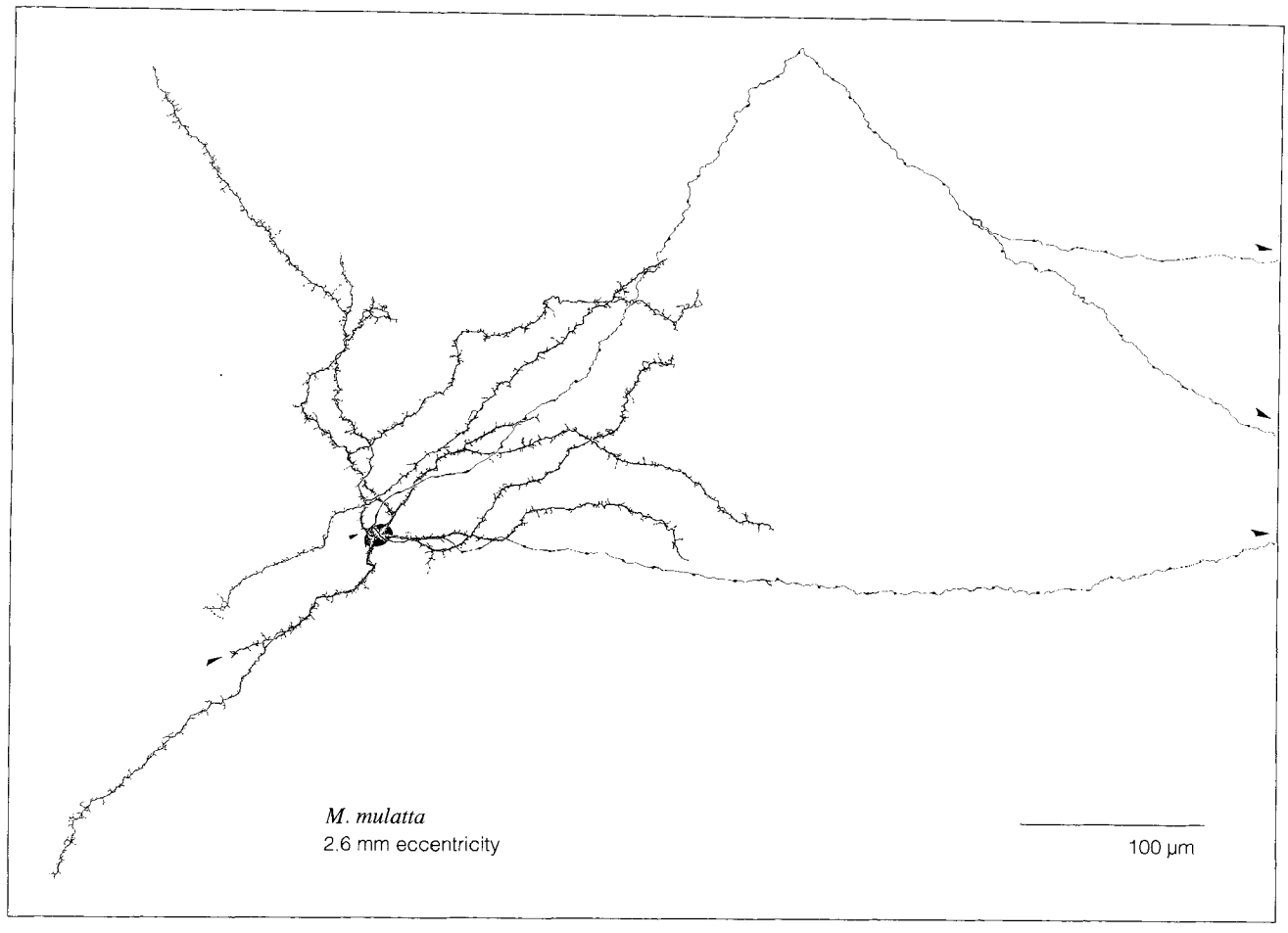

Fig. 6. Camera lucida tracing of the most centrally located DA-like amacrine cell in the sample of HRP-filled cells. A single axon-like process arises from a primary dendrite close to the cell body and bifurcates close to its origin (small arrowhead). The axon-like processes extended towards the fovea for ~1.5 mm before the HRP reaction product diminished. The dendritic tree and axon-like processes were narrowly stratified at the outer border of the inner plexiform layer. However, a single, anomalous dendrite (large arrowhead) ascended towards the ganglion cell layer and stratified at the inner border of the inner plexiform layer close to the ganglion cell layer. Arrowheads indicate axon-like processes continue beyond the field shown for 1–2 mm.

The dendrites of the DA-like amacrine cells all appeared to be narrowly stratified near the outermost border of the inner plexiform layer. Measurements of the depth of stratification for 103 cells, expressed as the percent of the IPL's thickness as measured from the ganglion cell layer, gave a range of depths from ~75 to 95% with a mean ± SD of 81 ± 5% (Fig. 9A). The dendrites of these cells thus appeared to span a narrow band that occupies approximately the outer 20% of the inner plexiform layer. The same result was also shown for two other cells using a computer system that preserved depth information. A 90° rotation of one of these cells confirmed the narrow stratification indicated in the histogram and illustrated that the dendrites remain in a narrow plane throughout their course (Fig. 9B). Rare exceptions were noted to this stratification pattern for individual dendritic branches of 3 cells in the sample. One such exception is a single branch of the cell illustrated in Figure 6 (large arrowhead) that turned sharply inward and stratified in the approximate center of the IPL.

The axon-like processes

The DA-like amacrine cell shown in Figure 2 illustrates the most common pattern for the origin of the axon-like processes from the dendritic tree: in 75% of the injected cells a single thin, axon-like process arose directly from the soma, and 1 to 3 similar processes typically arose from the dendrites close to the soma, proximal to the first dendritic branchpoint (see also Fig. 4A). Taking the axon-like processes that originated from the soma and the dendrites together, the cells showed a range of 1–4 axon-like processes (n = 114, mean ± SD = 2.4 ± 0.8). In 16 cells 1 or 2 axon-like processes arose from the soma only, and in 11 cells axon-like processes arose from the proximal dendrites only.

The morphology and branching pattern of the axon-like processes was strikingly different from that of the dendrites. They were relatively thin and smooth compared to the thick and spiny primary dendrites. It was not possible to accurately measure the thickness of these thin processes at the light microscopic level. They appeared to be slightly thickened (~0.5 μm diam.) for a short distance from their origin (~10–50 μm) and then tapered to a much finer diameter. These extremely thin and smooth processes were studded with distinct, large varicosities (~1 μm diam.). The axons remained unbranched or showed only one or two simple bifurcations. The total number of branches per cell

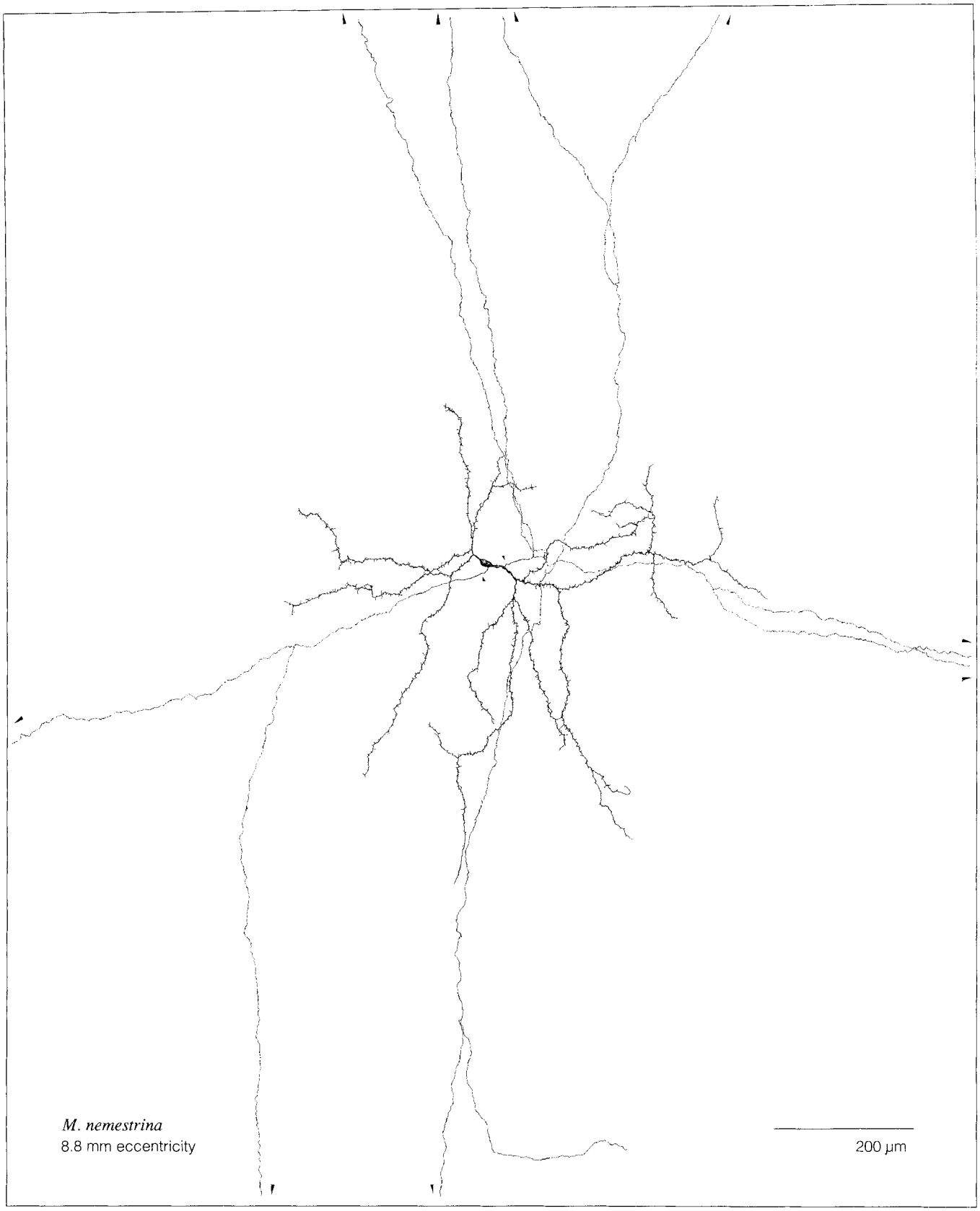

Fig. 7. Camera lucida tracing of a more peripherally located DA-like amacrine cell. Small arrowheads indicate the origin of the axon like processes from the somata and proximal dendrites. Large arrowheads indicate the continuation of the axon-like processes for 1–2 mm beyond the field shown. A photomicrograph of this cell is illustrated in Fig. 4A; a higher magnification camera lucida tracing is illustrated in Fig. 18B.

ranged from 6 to 11 (n = 99, mean ± SD = 8.5 ± 1.0). Overall the axon-like processes followed a relatively straight course away from their origin and their distribution can be best shown in a low magnification tracing (Fig. 3). However, between varicosities the axon-like processes followed a distinctly tortuous and wavy course that can best be observed at higher magnification (Figs. 2, 4).

Each axon-like branch extended beyond the dendritic field with the result that the total axonal tree was much larger than, and surrounded the parent dendritic tree. No axon-like branch was traced to an apparent termination as the HRP reaction product diminished in each branch typically between 1 and 3 mm from its origin. To estimate a minimum size of the axonal tree relative to the dendritic tree the longest process for each HRP-filled cell was taken as the radius of a presumed circular field (with a few exceptions [e.g., Fig. 6], the axons appeared to radiate in all directions from the dendritic tree, (e.g., Figs. 2, 7, and 18), so that the assumption of a symmetric axonal field is probably correct for most cases). The minimum axonal field was on average 6 times the diameter of the dendritic tree at all eccentricities examined (Fig. 10). The mean diameter for the minimum axonal tree was 3,000 ± 800 μm (n = 118, range = 1–5.4 mm) compared to a 500 ± 73 μm for the dendritic tree.

The axonal tree appeared to be narrowly stratified at the same depth as the dendritic tree, close to the inner nuclear layer border. Many axon branches were traced throughout their entire course and showed essentially no change in depth of stratification, remaining always within 1–2 μm of the plane of focus of the somata of the inner nuclear layer. The statification of the axon-like processes for all the cells in the sample was measured as described for the dendritic tree and is shown in Figure 9A. The axons showed a mean depth of 83 ± 4%, essentially matching the depth of stratification of the dendritic tree. Like the dendritic tree, the axonal fields of 2 cells were traced with the Eutectics system and rotated by 90° to give a picture of the overall stratification for a single cell (Fig. 9B).

There were some rare but noteworthy exceptions to the depth of stratification for the axonal field just described. In three cases a single branch of the axonal tree ascended

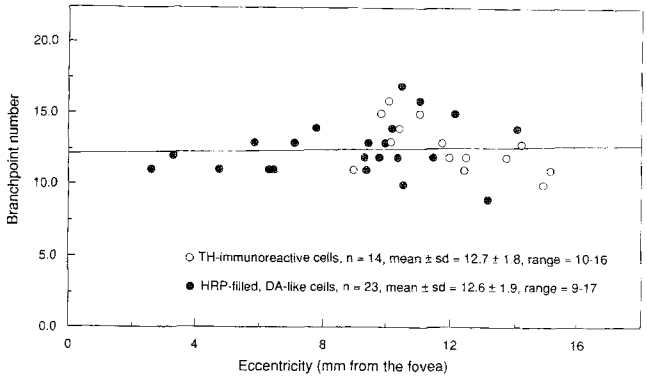

Fig. 8. The number of dendritic branch points for a sample of the HRP-filled DA-like amacrine cells and the large, TH-immunoreactive amacrine cells. The number of dendritic branchpoints for the DA-like cells indicated by the filled symbols remains constant with increasing eccentricity and increasing dendritic field size. Branchpoint number may thus be a fairly reliable size independent marker for this cell type. The branchpoint number for a sample of 14 TH-immunoreactive amacrine cells indicated by the open symbols (these were relatively rare cases in which the dendritic tree appeared to be stained completely) closely matched that of the DA-like cells (12.7 ± 1.8 μm) and also appeared to be a size independent feature.

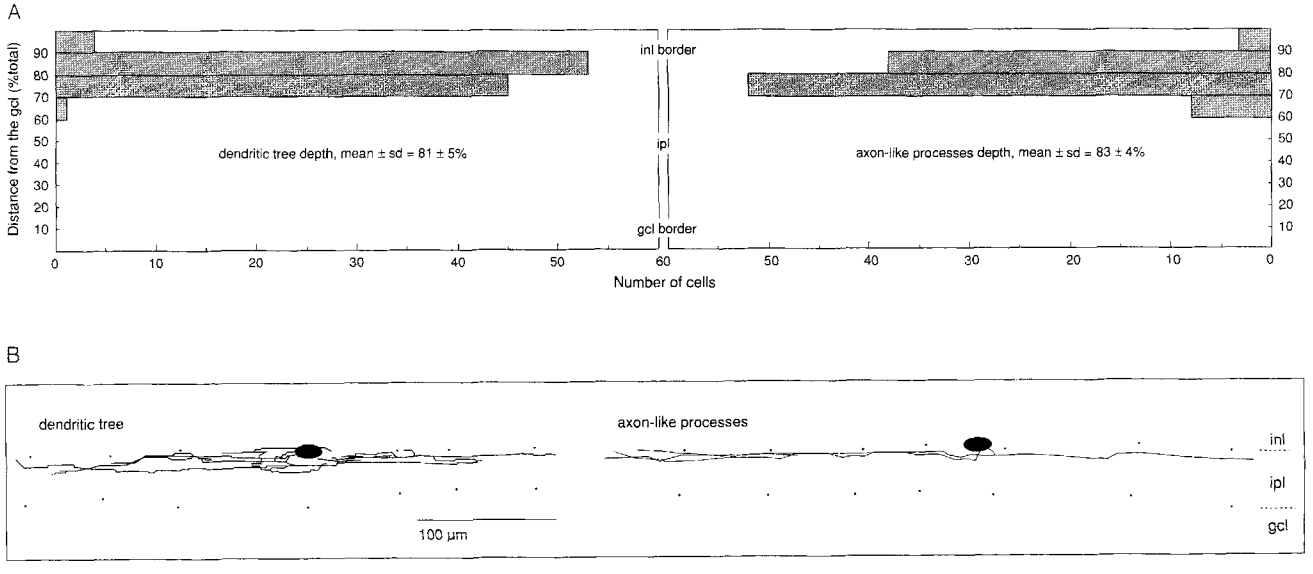

Fig. 9. Both the dendritic tree and the axon-like processes of the DA-like amacrine cells are narrowly stratified close to the outer border of the inner plexiform layer. **A:** Depth measurements of the dendritic tree (left) and the axon-like processes (right) were made relative to the inner nuclear layer and the GCL borders at a single location where the dendrites and axon-like processes were in close proximity by taking successive readings of the microscope focus knob (calibrated to 1 μm intervals). The results are expressed in the histogram as a percentage of the total thickness of the inner plexiform layer and confirmed that the dendritic tree and the axon-like processes are both narrowly stratified close to the outer border of the inner plexiform layer. **B:** A 90° computer rotation of a single DA-like amacrine cell. The portion of the axon-like processes that extends beyond the dendritic tree is not shown, but also maintained a narrow stratification close to the outer border of the inner plexiform layer.

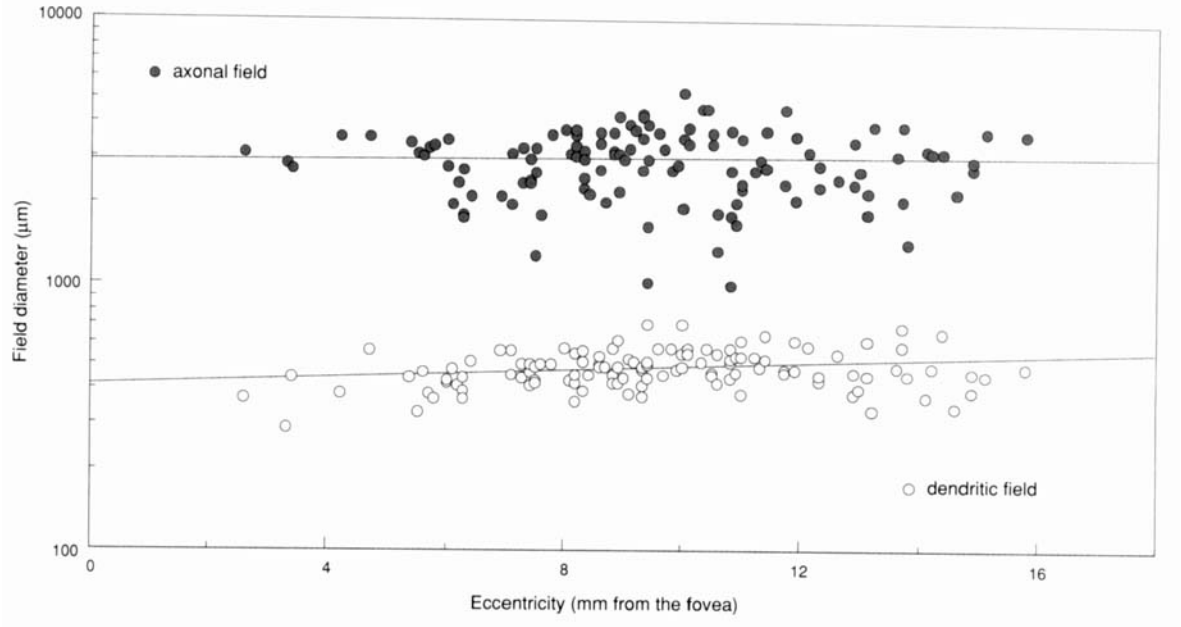

Fig. 10. Scatterplot of dendritic field and axonal field size as a function of retinal eccentricity for the DA-like amacrines. For each cell the axonal field size was plotted with the hatched circles and the dendritic field size with the open circles. Note that a logarithmic scale is used for the y-axis. For the dendritic field, n = 118, mean ± SD = 505 ± 83, range = 298–743. For the axonal field, n = 118, mean ± SD = 2,973 ± 824 μm, range = 1,000–5,380 μm. It is important to note that in no cases was it possible to trace the axon-like processes to an apparent termination so that the estimation of the axonal field size should be considered a minimum estimate. The lines through the two sets of points were fit by linear regression.

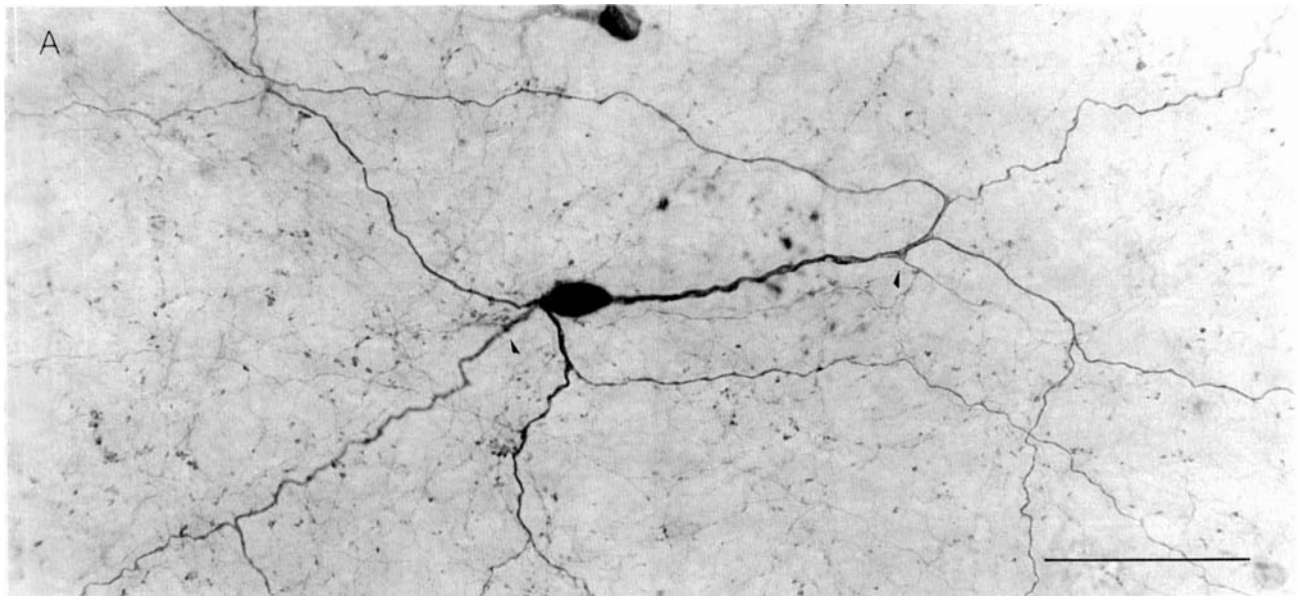

Fig. 11. Morphology of the large, intensely staining TH-immunoreactive cells. In most instances only the proximal dendritic tree of the TH-immunoreactive cells was stained intensely. However, in the periphery of a single well-stained retina 14 cells appeared to be stained in their entirety and to show their complete dendritic branching pattern. **A:** A single well-stained cell from peripheral retina. The thicker dendrites are more intensely immunoreactive than the varicose plexus in which it is embedded. The arrowheads indicate locations where two presumed axon-like processes arise from the primary dendrites. **B:** Camera lucida tracing of the cell shown in A illustrates the extent to which the dendritic tree could be observed. The two, lightly stained axon-like processes (small arrowheads) could be traced for a short distance before they were lost in the meshwork of fine varicose processes (larger arrowheads). The small arrowheads mark approximately the same locations in the photomicrograph and the tracing.

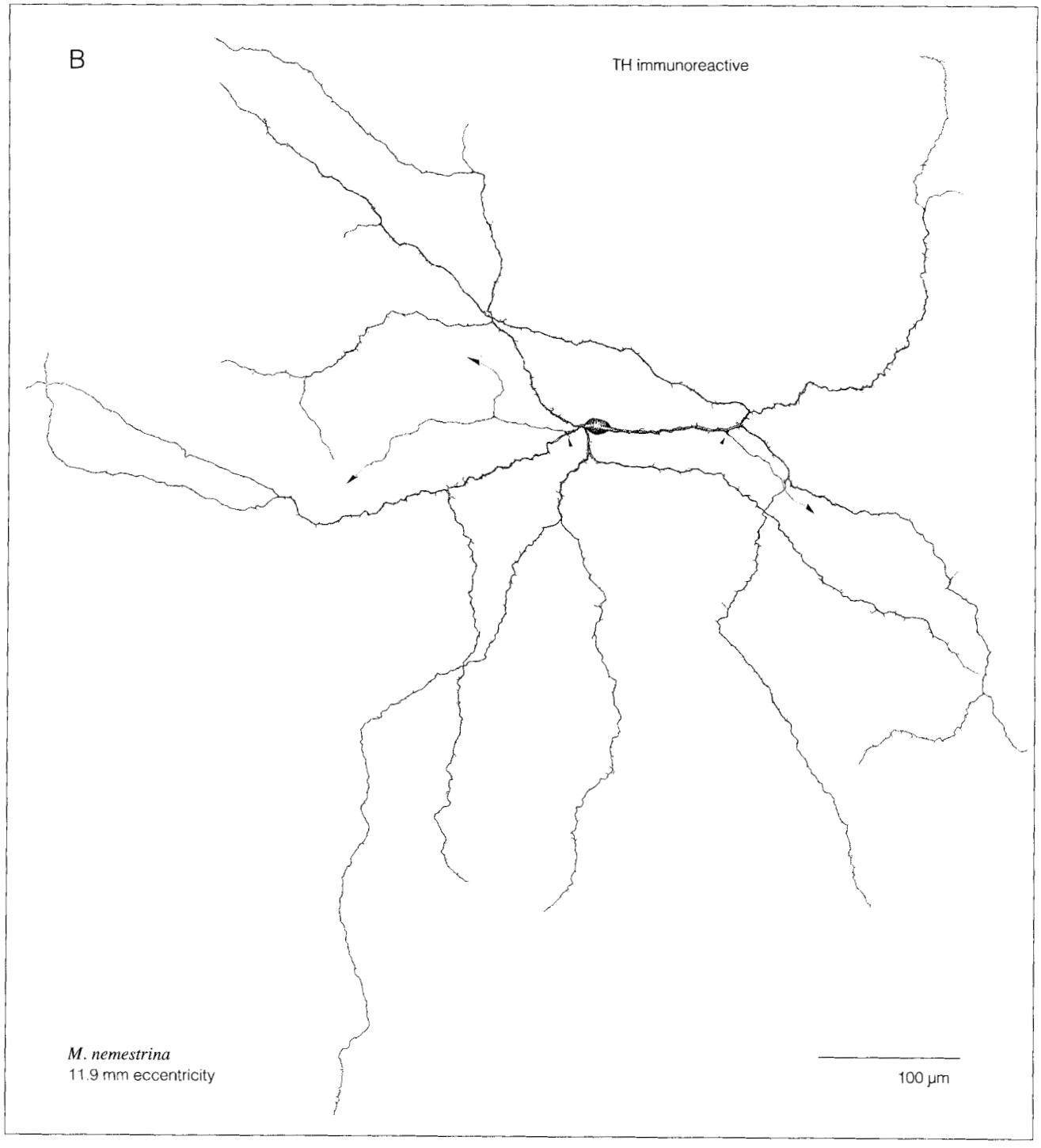

Figure 11 continued

through the inner nuclear layer, turned and extended for a few hundred microns at the inner border of the outer plexiform layer before it appeared to terminate. In one other case an axonal branch descended to the vitreal border of the inner plexiform layer and coursed for several hundred microns before ascending back to its original level of stratification. It is not clear whether these infrequent departures from the principal depth of stratification are present in each of the DA-like amacrines. The total extent of HRP-filled axon-like processes from many of the other cells in the sample were carefully followed under high magnification and did not show any change in stratification. However it is important to emphasize again that these axon-like processes were not HRP-filled in their entirety,

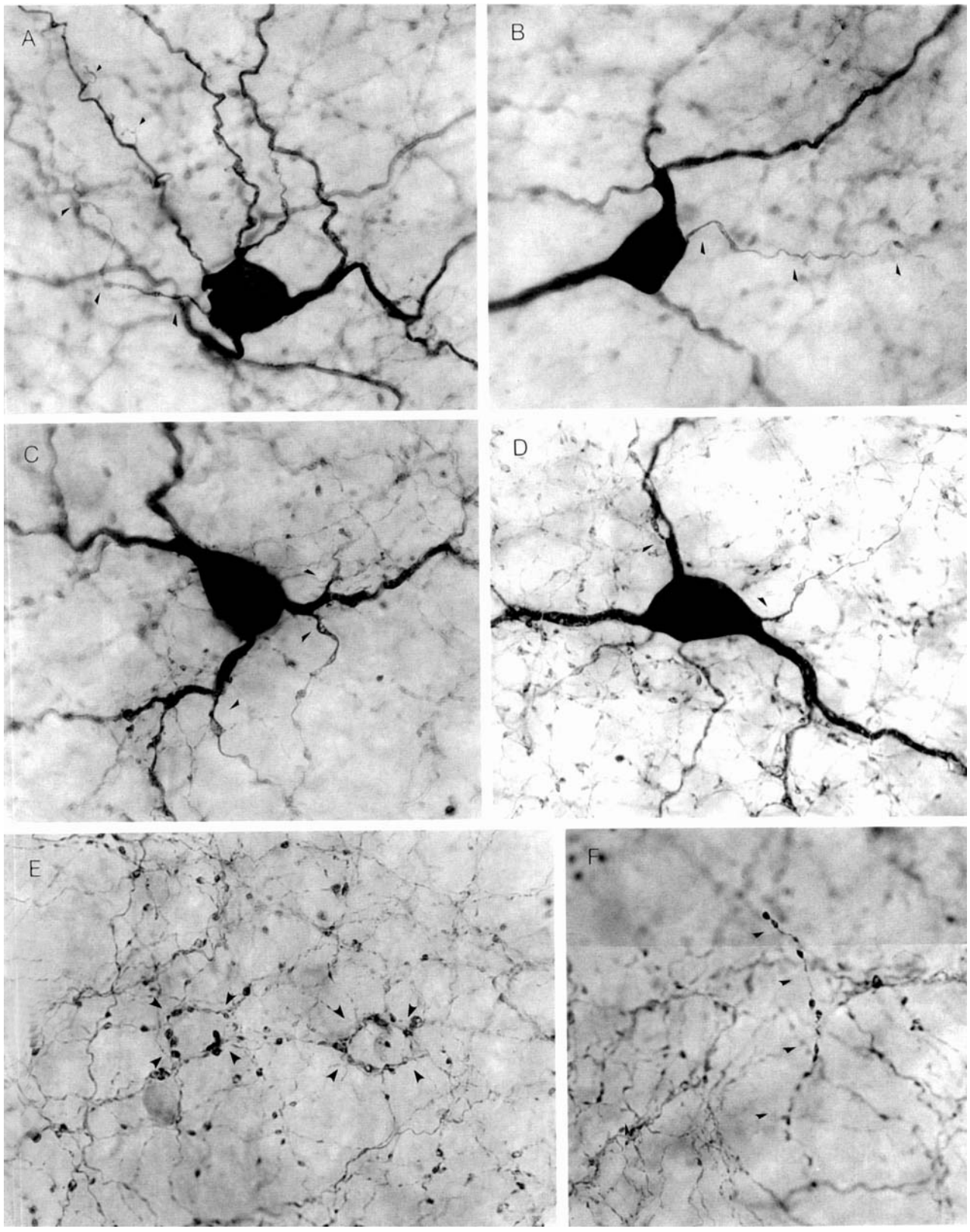

Figure 12

and it is therefore possible that a small, unfilled component of the axons of all of the cells did depart from the major level of stratification.

Evidence that the DA-like amacrines are dopaminergic

Several pieces of evidence suggest strongly that the DA-like amacrines are the large TH amacrine cells. For the great majority of immunoreactive cells, only the proximal portions of the dendritic tree were clearly observed. However in a few instances in the retinal periphery the entire dendritic tree appeared to be completely stained, and stood out against a more lightly stained plexus of fine processes (Fig. 11A). The overall dendritic branching pattern of 14 immunoreactive cells traced by camera lucida appeared indistinguishable from that of the DA-like cells. In addition both groups show nearly identical numbers of branchpoints (TH-immunoreactive: 12.7 ± 1.8; DA-like: 12.6 ± 1.9) and in both groups the number of branches were similar at all eccentricities (Fig. 8). Similarly, the dendritic field diameters of the 14 TH-immunoreactive cells were also highly overlapping with the DA-like amacrine cells (Fig. 13B). Although it is a small sample, the broad range of dendritic field diameters for the peripheral TH-immunoreactive cells was also similar to that of the HRP-filled cells.

The range of soma sizes for the DA-like amacrines also largely overlapped that for the TH amacrines (Fig. 13A). Soma diameter for the TH-immunoreactive cells was measured for all cells in a 1 mm wide strip running from the dorsal retinal periphery to the fovea. Soma diameter increased with eccentricity, ranging from 8 μm in the fovea to a maximum of 18 μm in the far retinal periphery. For the DA-like amacrines, soma diameter ranged from 11.1 μm at 2.3 mm eccentricity to 16.6 μm in the far retinal periphery. The means for both groups at the range of eccentricities where the samples overlapped was 13.5 ± 1.1 μm and 13.9 ± 1.5 μm for the DA-like amacrines and the TH-immunoreactive cells, respectively. The difference between these means (0.6 μm) although small was significant ($P < 0.02$). The small differences in both soma and dendritic field size are probably due to differences in how the tissue was fixed. The HRP-filled cells were fixed in 1% glutaraldehyde and the immunoreacted tissue was fixed in 4% paraformaldehyde.

The morphology of the dopaminergic amacrines revealed by tyrosine hydroxylase immunoreactivity revealed fine details that were directly comparable to the HRP-filled DA-like amacrines. Some of the dendrites of immunoreacted cells had complex spine-like structures that appeared to correspond to the spines on the dendrites of the DA-like cells (Figs. 11, 12). These dendritic details were not easily observed on most cells because the dendrites were typically obscured by the costratified plexus of fine processes and also because the preservation of detailed morphology is often not good in immunoreacted tissue due to the use of detergents to enhance antibody penetration. Occasionally, however, spines were clearly observed on well-stained dendrites that were slightly displaced from the intensely staining plexus at the outer border of the IPL (Figs. 11, 12A).

Perhaps the strongest indirect evidence that the DA-like amacrine cells and the TH-immunoreactive cells are the same was the observation that at least one axon-like process was observed arising from the soma of almost every well-stained TH-immunoreactive cell (Figs. 11, 12). The axon-like processes were extremely thin and varicose and often traced for a short distance before they were lost in the meshwork of other immunoreactive processes. The axon-like processes were most clearly revealed on immunoreactive cells that were displaced into the ganglion cell layer (Figs. 11, 12A,B). In all well stained displaced cells a thin process was observed arising from the soma and extending to the outer border of the IPL where it eventually joined the main plexus and could not be followed further. The axon-like processes were thus more easily observed on these cells simply because they traversed a portion of the IPL that contained few other processes. Possible axon-like processes also appeared to originate from the proximal dendrites of the normally placed cells (Fig. 12C,D), although this observation was made with less certainty because of the dense plexus that overlapped the dendrites.

The most direct evidence for the equivalence of the DA-like amacrines and the TH-immunoreactive cells comes from double labeling experiments. In these Lucifer Yellow that had been injected into the large acridine-stained amacrines was colocalized with TH immunoreactivity (Fig. 14). After the injection of Lucifer Yellow cells were then photographed either while still in vitro or after fixation. The tissue was then processed for TH immunoreactivity. In some cases both the Lucifer Yellow and the TH reaction product could be seen in the same cells. In other cases the TH reaction product was so intense that it blocked visualization of the Lucifer Yellow in the cell. In these cases verification of the double labeling was possible by comparing the dendritic branching pattern of the TH-immunoreacted cell with the photograph of the Lucifer Yellow-filled cells taken before immunohistochemistry (Fig. 14). All cells (n = 21) that had a DA-like morphology could be double labeled in this way. Several cells that were injected with Lucifer Yellow but showed a morphology and stratification distinct from the DA-like cells were not double labeled.

Calculation of independent dendritic and axonal tree coverage

Given that the DA-like amacrines are the same as the TH amacrines, it is possible to use the cell densities in the

Fig. 12. Morphological details of the intense TH immunoreactivity in *M. nemestrina* retina. The features of the morphology of the DA-like amacrines can also be observed in TH-immunoreacted retinal wholemounts. **A,B:** Immunoreactive cells that are displaced into the ganglion cell layer permit observation of dendrites and axon-like processes as they extend outward through the inner plexiform layer. Thin axon-like processes arise from the somata of these two cells (arrowheads) and could be traced to the outer border of the inner plexiform layer where they joined the major immunoreactive plexus. Distinct spines were also sometimes observed on the dendrites (small arrowheads). **C,D:** Axon-like processes (arrowheads) could also consistently be observed arising from the great majority of immunoreactive somata in the inner nuclear layer. These processes could not be traced for any great distance as they quickly were lost in the meshwork of fine processes at the outer border of the inner plexiform layer. **E:** The immunoreactive plexus is created by a high density of fine varicose processes. Clusters of varicosities sometimes outline the apparent somata of unstained cells that protrude into the inner plexiform layer (small arrowheads). **F:** A small number of fine varicose processes leave the main plexus in the inner plexiform layer and extend into the inner nuclear layer and the inner border of the outer plexiform layer where they appear to terminate. One such process is indicated here by the arrowheads.

immunoreacted retinas to calculate the overlap for both the dendritic and axonal fields of the HRP-filled cells. Figure 15 shows the topographic map of spatial density for the large, intensely staining TH-immunoreactive cells in a single retina. Cell density ranged from ~10 cells/mm^2 in the far periphery to a peak of 50 cells/mm^2 in the central retina.[1] Cell density peaked around the foveal pit at about 0.5 mm eccentricity; no immunoreactive neurons were observed in the base of the foveal pit. The shape of the isodensity contour lines were roughly circular and symmetric around the fovea. There was some indication of a nasotemporal asymmetry suggested by a slightly higher cell density in the temporal periphery. Only one retina was sampled completely; 9 other TH-immunoreacted retinas were available for study and all showed qualitatively the same density gradient, although it is not clear whether the slight spatial asymmetries in this map represent a characteristic feature or reflect individual variation.

Figure 16 shows a camera lucida tracing of the dendritic tree and the axon-like processes of an HRP-filled DA-like amacrine superimposed on the mosaic of large, TH-immunoreactive cells. It is evident from this picture that the population of dendritic trees will overlap much less than the longer axon-like processes. The mean dendritic field diameter for the DA-like cells was ~500 μm. A mean density of 14 cells/mm^2 for the TH-immunoreactive cells gives a mean coverage of 2.7. The smallest DA-like cells in the sample showed a dendritic field diameter of ~350 μm at 2–4 mm eccentricity. The TH cell density of ~25–35 cells/mm^2 at this eccentricity gives a coverage of 2.4–3.4. The largest cells showed a field diameter of ~700 μm at about 15 mm eccentricity. A TH cell density of ~5–10 cells/mm^2 at this eccentricity gives a coverage of 1.9–3.8. Thus the shallow density gradient across the retina for the TH-immunoreactive cells is in inverse relationship with the equally small change in dendritic field size for the HRP-injected sample; the result is a roughly constant coverage from central to peripheral retina. This degree of dendritic overlap is characteristic of other amacrine and ganglion cell types whose cell bodies show a regular spacing and whose dendritic trees partially overlap (e.g., Wässle et al., '81; Vaney, '85; Buhl and Peichl, '86; Dacey, '89b). No neighboring DA-like cells were injected with HRP in this study. However, given the narrow stratification and sparse branching pattern, it is possible that the overlapping dendrites of neighboring cells could interdigitate and show a high degree of local order. Such a situation has been documented for the overlapping dendritic trees of a single ganglion cell type in the cat's retina (Dacey, '89b).

In contrast to the dendritic fields, the fields formed by the long axon-like processes must overlap extensively (see Fig. 10). The longest HRP-filled axonal process in the sample was traced for 2.7 mm before the reaction product diminished, giving a minimum axonal field diameter of 5.4 mm. This would give a minimum coverage of ~320 in mid-peripheral retina at cell densities of 14 cells/mm^2. (If axonal field diameter does not increase positively with eccentricity then coverage would increase to ~1,000 in the central retina and decrease to ~200 in the far retinal periphery. The TH-immunoreactive plexus appears to show such a central to peripheral decrease in density, although this change was not directly measured in this study.) The axonal field coverage is thus at least 100 times that of the dendritic field and would be expected to produce a meshwork of varicose, overlapping processes that costratify with the distinct territories formed by the partially overlapping dendritic trees. This pattern is essentially what is observed in the TH-immunoreactive wholemounts. Figure 17 illustrates how this dual pattern can be graphically simulated from the morphology of single DA-like amacrines.

Equivalence of axonal tree and TH immunoreactive plexus

If the axonal trees of the DA-like amacrines correspond to the fine, varicose TH-plexus, then the calculated overlap of the axonal trees should produce a density of processes that is equivalent to that present in the TH-immunoreacted retinas. However, because the axon-like processes were not filled completely by the intracellular HRP injections, a calculation of the density of processes based on the filled cells must be an underestimate. This logic would predict that the density calculated from the axonal processes of the HRP-filled cells should be somewhat less than the actual density of the TH plexus and that the difference between the two values should provide some indication of the true length of the axon-like processes.

The actual density of the TH plexus was estimated by making camera lucida tracings of all of the fine varicose processes in several 100 μm^2 fields at a retinal eccentricity of 10 mm. The total length of these processes was found for each of 10 fields; the mean length was 380 ± 30 mm/mm^2. This value was compared to the density calculated for the axon-like processes of the HRP-filled cells at 10 mm eccentricity which was ~130 mm axon/mm^2. (The mean of 8.5 axonal branches/cell was multiplied by the mean length of 1.5 mm for an axonal branch to give an average length of 12.8 mm of axon/cell.) Thus the density expected from the partially filled axons is only about one-third that of the density in the actual TH plexus. This suggests that each axonal branch must actually be on the order of 4–5 mm long to fully account for the density of the TH plexus.

The morphological properties of the macaque dopaminergic amacrine cells determined from the sample of HRP-filled cells and the spatial density demonstrated by TH immunoreactivity are summarized in Table 1.

DISCUSSION

The morphology of the dopaminergic amacrine cell

The dopaminergic amacrine cells of the macaque retina give rise to multiple, axon-like processes that spread widely beyond the dendritic tree. Similar dendritic and axon-like components were recently identified on a monoamine-accumulating amacrine cell type in the cat's retina, and it was suggested that these neurons were equivalent to the large dopaminergic amacrines (Dacey, '88, '89b). However,

[1]A previous observation of catecholamine histofluorescence suggested a trough rather than a peak in the density of the large dopaminergic amacrine cells in the perifoveal region (Mariani, et al., '84). By contrast, subsequent studies using TH immunohistochemistry suggested that the peak density of these cells lies around the foveal pit in macaque, and in the area of highest ganglion cell density in other mammalian retinas (review: Nguyen-Legros, '88). In some macaque retinas I have observed an apparent decrease in the TH immunoreactivity within 3 mm of the fovea, but this result appeared to be an artifact due to the lack of antibody penetration in a part of the retina where the optic fiber layer and ganglion cell layer are relatively thick. This effect dissappeared when higher antibody concentrations and longer incubation times were used. A similar problem might account for the results of Mariani et al. ('84).

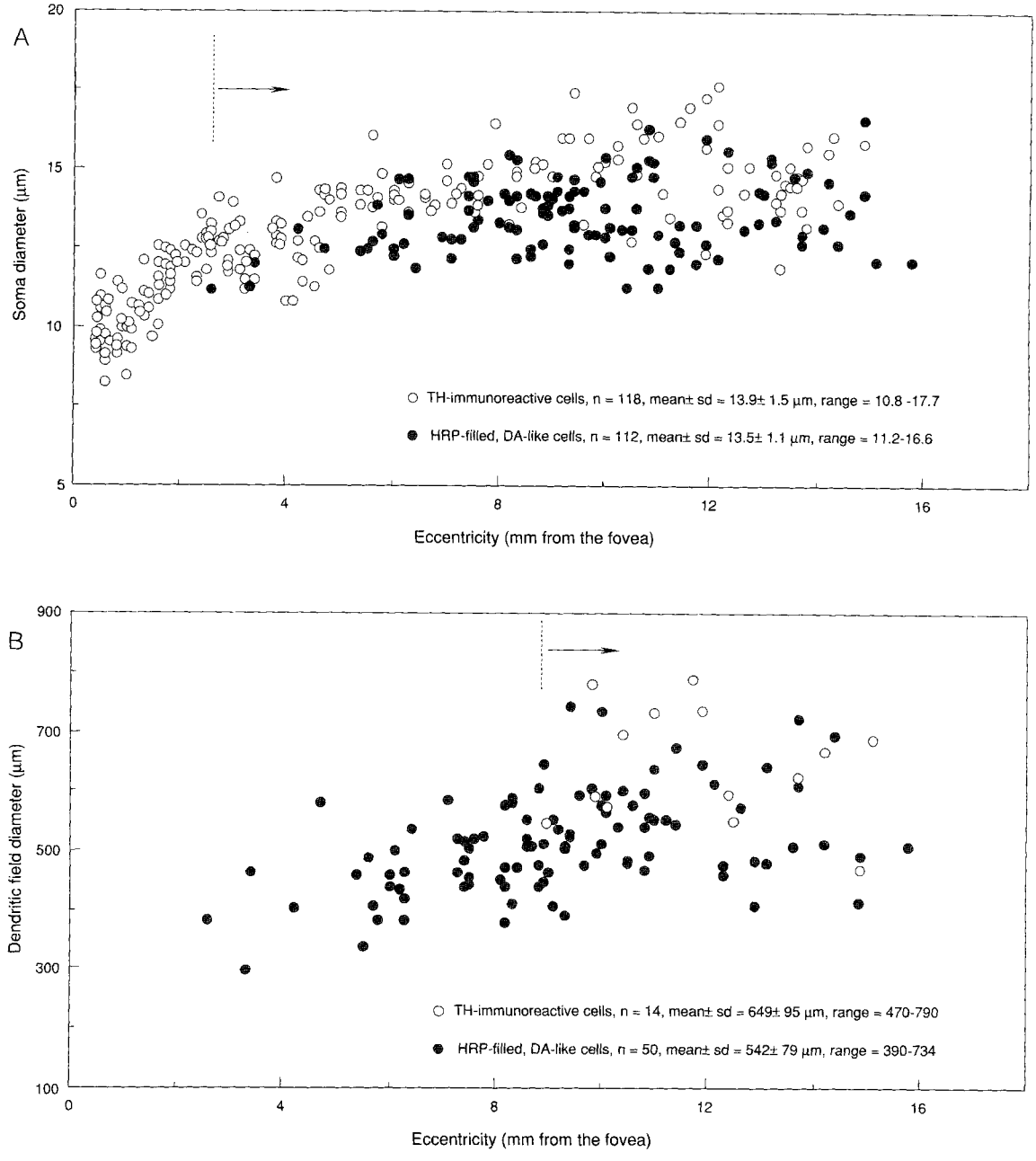

Fig. 13. Scatter plots comparing soma size and dendritic field size of the DA-like amacrines with the TH-immunoreactive cells. **A:** Soma size for the large, intensely staining TH-immunoreactive cells was measured from cells within a single, 1 mm wide transect extending from the dorsal periphery to the fovea. Size range for both groups is highly overlapping. However, the TH-immunoreactive cells showed a slightly larger (13.9 vs. 13.4 μm) mean size that was statistically significant ($P < 0.02$). **B:** Dendritic field size for the TH-immunoreactive cells could not be systematically measured because the great majority of cells were only partially stained. However, in 14 instances in the retinal periphery staining of the dendritic tree was very intense and appeared to be complete. (One such "completely" stained cell is illustrated in Fig. 11.) As for the soma size the TH-immunoreactive cells showed a highly overlapping but slightly larger dendritic field size ($P < 0.01$). The DA-like cells were compared to the subset of TH-immunoreactive cells only over the retinal eccentricities where the two groups overlapped. This region is indicated by the dotted line and the arrow in both A and B.

a detailed comparison shows clearly that they are morphologically distinct cell types (Fig. 18A,B). The main dendrites of the cat monoamine-accumulating amacrine cells bear a number of distinct branchlets. The main dendrites of the macaque amacrine, though spiny, rarely give off dendritic side branches. More significantly, the majority of axon-like processes of the cat monoamine-accumulating amacrines arise by an abrupt tapering of the principal dendrites (arrowheads, Fig. 18). In striking contrast, the comparable axon-like processes of the macaque dopaminergic cells arise from the soma and the proximal dendrites.

The morphological differences between the cat monoamine-accumulating amacrine cells and the macaque dopaminergic amacrine cells do not reflect species differences in

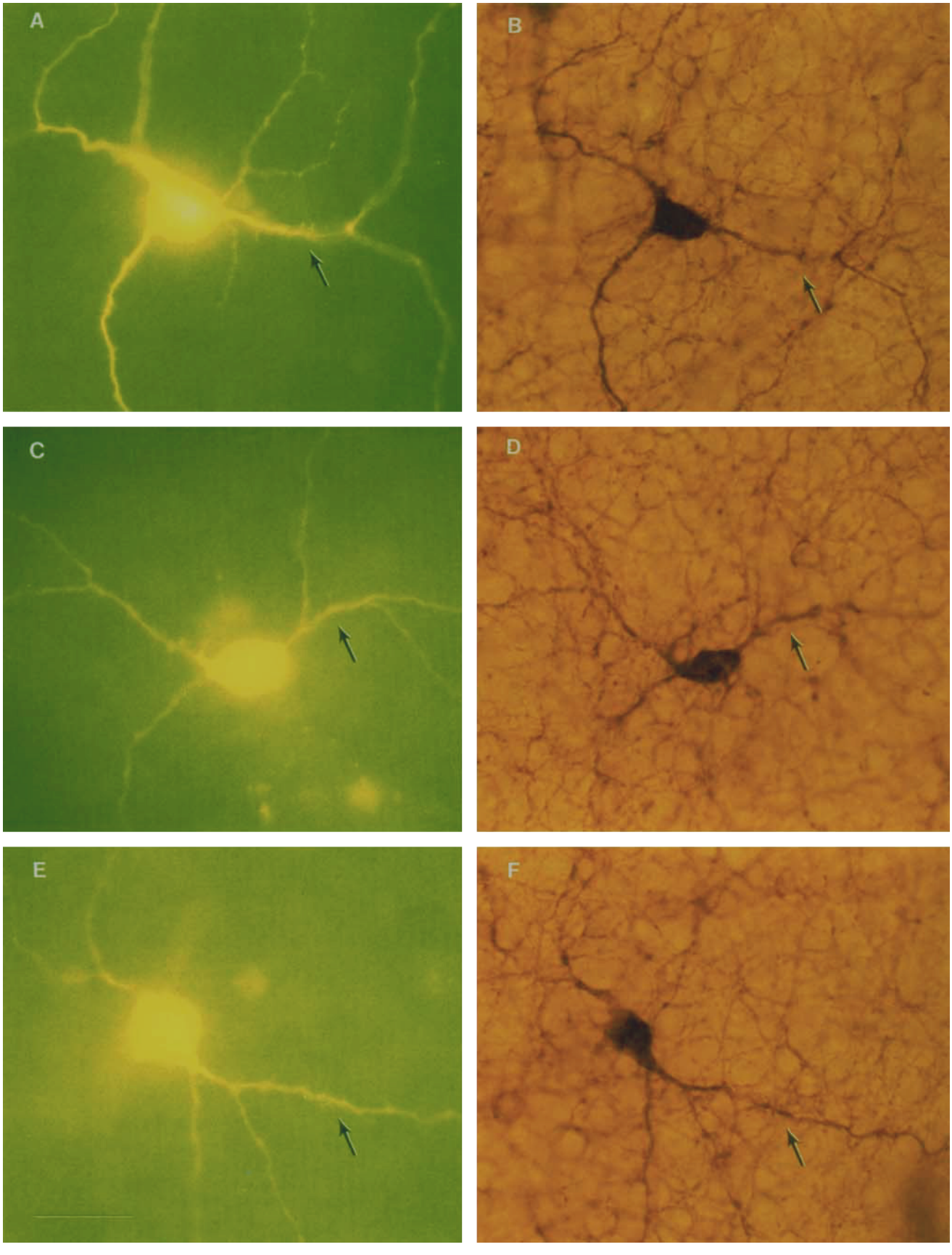

Figure 14

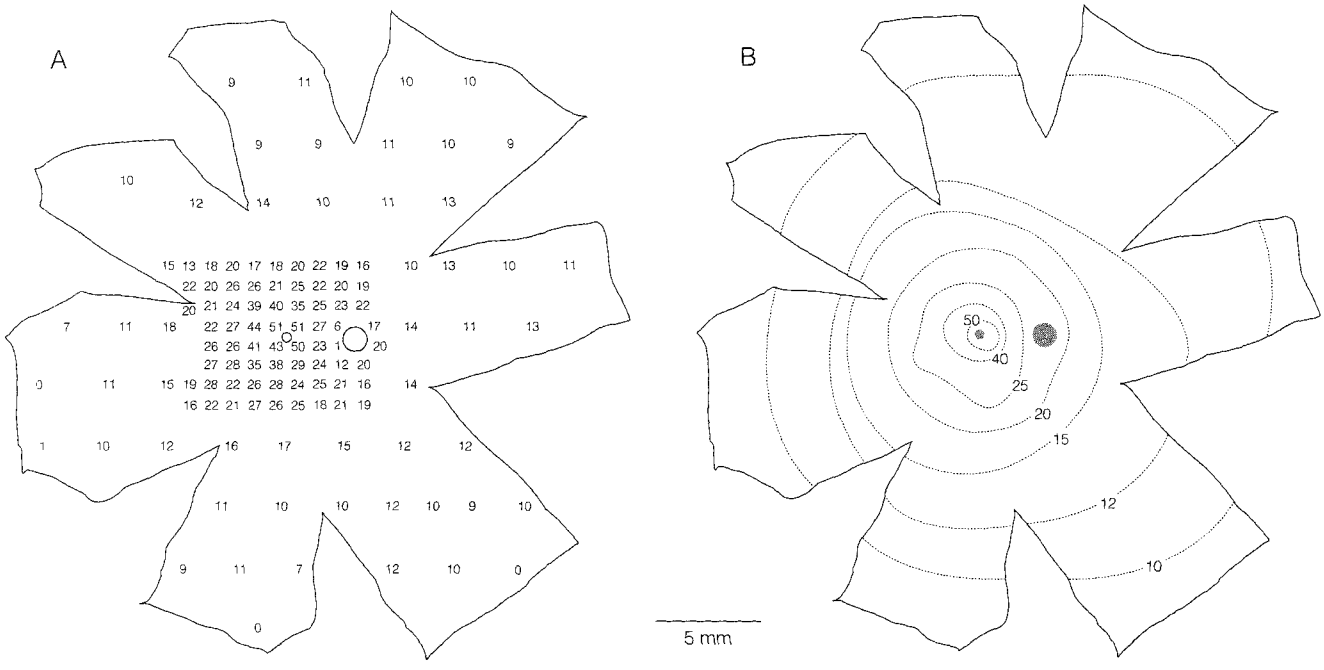

Fig. 15. Spatial density of the large, intensely staining TH-immunoreactive cells in *M. mulatta* retina. **A:** Map of actual cell counts made in 1 mm² areas. Adjacent fields were counted in the central 4 mm of retinal but counts were separated by 2 mm intervals in the retinal periphery. **B:** Isodensity map of TH cell topography derived from the counts shown in A. A peak density of 50 cells/mm² is reached at the fovea. Density is roughly symmetrical around the fovea and declines gradually to about 10 cells/mm² in the far periphery. Isodensity contour lines were interpolated by eye.

equivalent cell types. The cat monoamine accumulating cells do not show intense TH immunoreactivity[2] (Dacey, unpublished observations), and another amacrine cell type in the cat has recently been identified that shows the same morphological features as the macaque dopaminergic amacrine and can also be double labeled for TH immunoreactivity. (Dacey, '90; Fig. 18C). Like the macaque dopaminergic amacrine, it is sparsely branching and shows long axon-like processes that arise from the soma and the proximal dendrites. Both the dendritic tree and the axonal tree are narrowly stratified at the outer border of the IPL. Differences do exist between the cat and macaque dopaminergic cell types in their dendritic field size, density of dendritic spines, and in the branching pattern of the axon-like processes.

Other attempts to determine the morphology of the large, dopaminergic amacrine cells in cat (Voigt and Wässle, '87) and rabbit retina (Tauchi and Masland, '88) did not detect the distinct axon-like component reported here in the monkey. In these earlier studies neurons that exibited catecholamine histofluorescence in formaldehyde-fixed tissue were injected with Lucifer Yellow. Large amacrine cells that showed the same primary dendritic branching pattern observable by TH immunoreactivity were observed. The failure to detect the axon-like component may have been due to the difficulty of filling long, thin processes with Lucifer Yellow in fixed tissue (Voigt and Wässle, '87). In one instance fine, varicose processes were observed in the vicinity of the dendritic field, but the authors suggested that they arose as short side branches from the dendritic tree (Voigt and Wässle, '87, their Fig. 8).

Dopaminergic amacrine and interplexiform cells: variation in a single morphological type

The distinct dendritic and axon-like components may provide an important insight into the relationship between dopaminergic amacrine and interplexiform cell types. The TH-immunoreactive wholemounts in the macaque showed a very low density of intensely staining, fine, varicose processes in the inner nuclear and outer plexiform layers as previously observed in radial sections (Ryan and Hendrickson, '87). These processes could often be traced into the

[2] The neurotransmitter(s) of the cat monoamine-accumulating amacrine cell remains unknown. The morphology of these cells appears equivalent to one type of indoleamine accumulating amacrine identified recently in the cat's retina (Voigt and Wässle, '87). These sparsely branching cells were referred to as spiny amacrines and evidence has been given that they are GABA immunoreactive (Wässle and Chun, '88). It remains possible however, that the monoamine-accumulating amacrine cells also contain a catecholamine. The number of putative catecholaminergic cell types is not restricted to the large, intensely staining amacrine cells that stratify predominantly at the outer border of the IPL. Other, less intensely staining TH-immunoreactive cell types have been observed in the monkey (Mariani and Hokoc, '88; Dacey, unpublished observations) and rat retina (Versaux-Botteri et al., '86). In the rabbit retina 3 distinct catecholaminergic amacrine cell types have been suggested (Tauchi and Masland, '88). It is not known whether any of these cell types correspond to the monoamine accumulating cells.

Fig. 14. Demonstration of TH immunoreactivity in the DA-like amacrine cells. The large amacrine cells identified by acridine fluorescence were injected with Lucifer Yellow and photographed after fixation. The tissue was then processed for TH immunoreactivity as described in Materials and Methods. The same cells were again photographed. In all cases the DA-like amacrines showed intense immunoreactivity in both cell body and proximal dendrites. The Lucifer Yellow fluorescence is shown on the left (**A,C,E**) and the corresponding TH immunoreactivity is shown in the right column (**B,D,F**). Approximately the same location for each pair is indicated by the arrows.

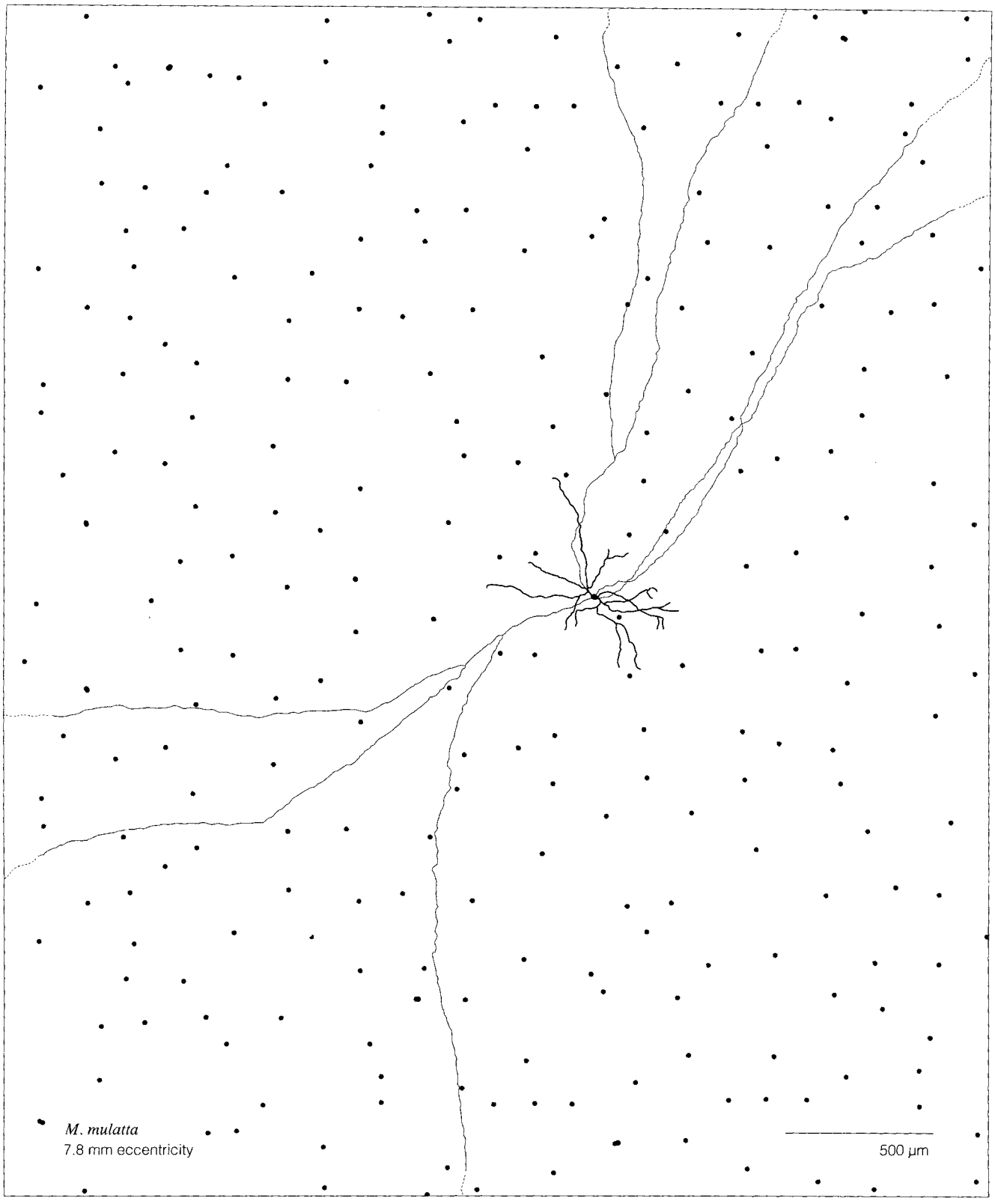

Fig. 16. The dopaminergic amacrine cell placed within the mosaic of TH-immunoreactive cell bodies. In this illustration an HRP-filled DA-like amacrine cell is placed within the mosaic of intensely TH-immunoreactive amacrines. The mosaic and the HRP-filled cell shown are taken from the retinal periphery about 10 mm from the fovea. TH-immunoreactive cells are plotted as the filled dots. The dendritic tree of the dopaminergic amacrine is traced by the heavy lines and the axon-like processes are shown by the thin lines. Note that the overlap of processes created by the extremely long axon-like processes would be many times that created by the dendritic trees. The axon-like processes of this cell could not be traced to a termination and their probable continuation is indicated by the dotted lines at the end of each process.

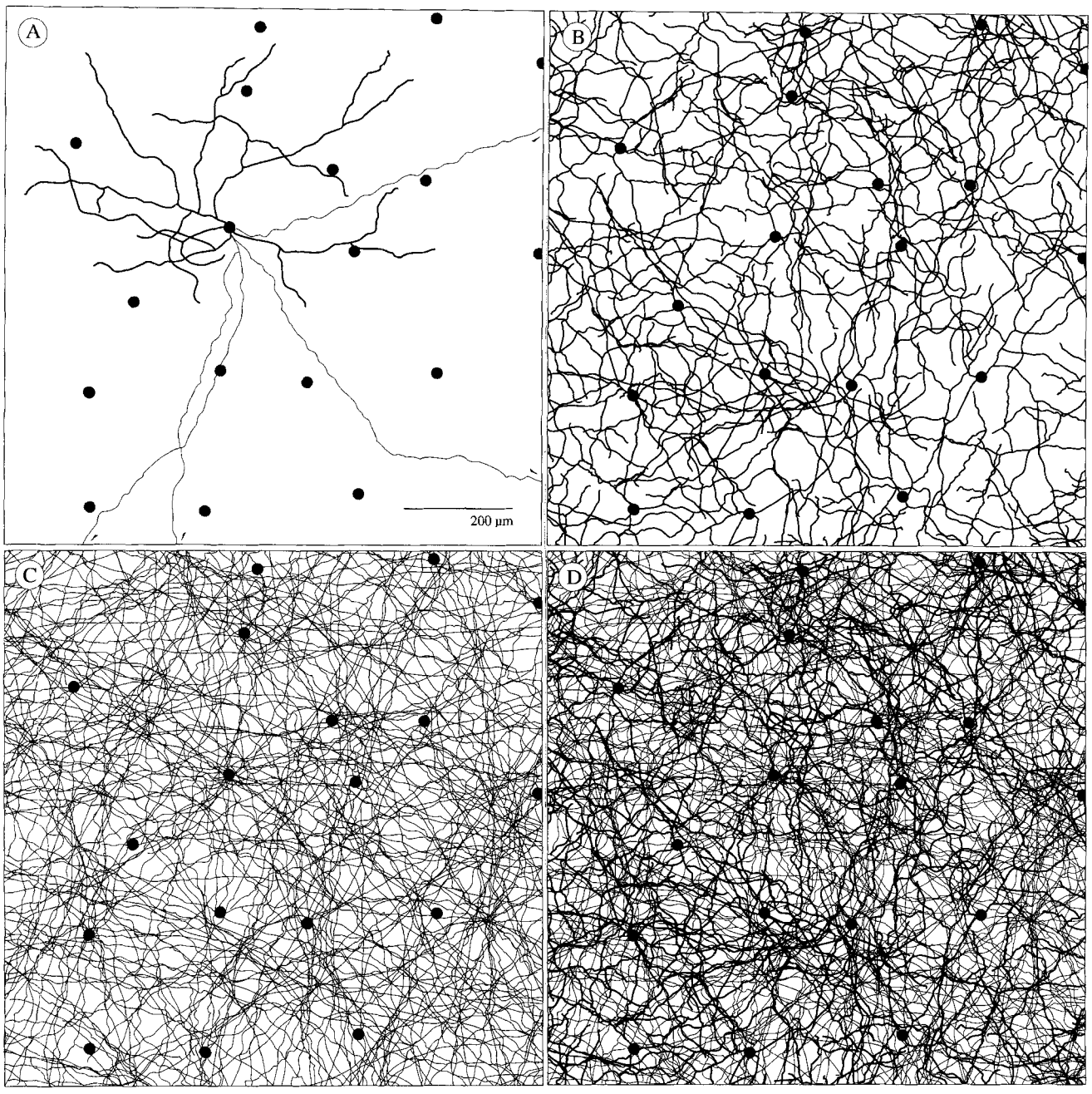

Fig. 17. Graphical simulation of the TH-immunoreactive plexus at the outer border of the inner plexiform layer from single HRP-filled dopaminergic amacrine cells. The same small patch of TH-immunoreactive cell bodies is represented by the filled circles in each of the four panels of this figure. **A:** A tracing of the branching pattern of the dendritic tree (thick lines) and axon-like process (thin lines) of a dopaminergic amacrine cell is superimposed on the mosaic. The small arrowheads indicated that the axon-like processes extend beyond the panel. **B:** The dendritic trees only of four HRP-filled cells are superimposed on the mosaic. Each cell was replicated a number of times, randomly rotated, and placed into the mosaic. The result provides a picture of the extent to which the dendritic trees alone contribute to the TH-immunoreactive plexus and how the calculated coverage would appear. **C:** Here the same process is repeated as in B but only the contribution of the axon-like processes to the plexus are now illustrated. **D:** Here the dendritic and axon-like processes are superimposed to give the entire plexus, which appears much like that observed in the TH immunoreacted wholemounts (Fig. 12). Note that given the possibility of longer axon-like processes that the axonal-plexus could be much more dense than that illustrated here. Also the coverage of the dendritic trees may in reality be more ordered and territorial with individual dendrites interdigitating and filling space more evenly.

dense TH plexus at the outer border of the inner plexiform layer where they appeared to originate (Fig. 12F). The HRP-fills of the dopaminergic amacrines suggest a clear basis for this pattern: in three instances a single branch of an axon-like process was followed from the inner plexiform layer to the outer plexiform layer where it appeared to terminate. The sparse TH-immunoreactive processes in the outer plexiform layer apparently correspond to the axon-like component of the large dopaminergic amacrine. The rare occurrence of outwardly directed branches in the

HRP-fills would thus explain the low density of processes in the outer plexiform layer relative to the inner plexiform layer. Similar observations have been noted in the TH-immunoreacted cat retina and a similar conclusion was drawn by Voigt and Wässle ('87). These observations, together with the lack of evidence for a separate population of dopaminergic interplexiform cells in the macaque suggests that the classically recognized dopaminergic amacrine is in fact equivalent to the interplexiform cell. It should be noted, however, that in the cat evidence has also been given for independent populations of dopaminergic amacrine and interplexiform cells (Oyster et al., '85; Takahashi, '88).

Current knowledge of the detailed morphology of the dopaminergic interplexiform cell in the teleost retina reveals a striking parallel with that of the dopaminergic amacrine shown in the present study (Fig. 19). The teleost interplexiform cells occur at a low spatial density and show large, sparsely branching dendritic trees (Negishi, '81; Teranishi and Negishi, '88). The outwardly directed processes originate from the soma and/or the proximal dendrites close to the soma. By contrast to the thick and spiny primary dendrites these processes appear extremely thin and smooth and bear distinct, presynaptic varicosities (Teranishi and Negishi, '86, '88). The extent of their course in the outer plexiform layer has not yet been determined, but the similarity of the outer plexiform layer directed processes of the interplexiform cells to the distinct axon-like processes of other teleost amacrine cell types has recently been noted (Teranishi and Negishi, '88). The overall pattern suggests that the dopaminergic amacrine cell and the dopaminergic interplexiform cell of teleost fish represent equivalent cell types that vary quantitatively across species in the degree to which the morphologically distinct axon-like processes extend into the outer retina.

The hypothesis that the dopaminergic amacrine corresponds to the interplexiform cell makes several clear and testable predictions. 1) *Distinct subpopulations of the large dopaminergic and interplexiform cell types should not coexist in the same retina.* That is, the large intensely TH-immunoreactive cells in all vertebrate retinas comprise a single, morphologically and functionally distinct subpopulation. It should be noted, however, that other catecholaminergic amacrine cell types, and other non-dopaminergic interplexiform cell types, may coexist in the same retina. 2) *Intermediate forms should exist in different species.* For example, the large TH-immunoreactive cell type in the rat's retina should show the same basic morphological features as the macaque and the cat dopaminergic amacrine. But because the dopaminergic innervation of the outer plexiform layer appears relatively more extensive in rats (Nguyen-Legros et al., '81; Negishi et al., '85; Savy et al., '89), it would be predicted that identified axon-like processes of a rat dopaminergic amacrine would show a correspondingly heavier projection into the outer plexiform layer. This hypothesis can be directly evaluated by intracellular HRP injection of identified rat dopaminergic amacrines. 3) *The axon-like processes of the dopaminergic amacrine should be strictly presynaptic, regardless of location in the inner plexiform or the outer plexiform layer.* If the axon-like processes are structurally and functionally equivalent across species, then the presynaptic nature of the outer plexiform layer projecting processes of the interplexiform cells predicts the same pattern for the corresponding processes of the amacrine cell. Likewise, the spiny dendritic tree of the dopaminergic amacrine should be the site of major synaptic inputs (and some synaptic output) as has been demonstrated for the dopaminergic-interplexiform cells. Supporting evidence for these predictions is discussed in the next section. 4) *The outer plexiform layer-directed processes of the teleost interplexiform cell should extend for long distances beyond the dendritic field.* As for the axon-like processes of the dopaminergic amacrine, it might be expected that the teleost outer plexiform layer-projecting processes of a single cell give rise to a sparsely branching axon-like tree that extends for several mms beyond the location of synaptic inputs to the dendritic tree. Consequently, the dense nest of dopaminergic boutons that contact the somata of cone horizontal cells would arise by convergence from a large number of parent cells distributed widely over the retina. Similarly, it might be expected that the outwardly directed processes of teleost interplexiform cells will show a minor component that extends into the inner plexiform layer and makes synaptic contact with other amacrine cell types. This prediction can be directly evaluated by intracellular filling of teleost dopaminergic-interplexiform cells with HRP.

The interplexiform cell is considered a unique class of retinal neuron in that it transmits information centrifugally from the inner to the outer plexiform layers. The evidence for centrifugal information flow is anatomical: synaptic inputs are restricted to the processes in the inner plexiform layer, and the processes in the outer plexiform layer give rise only to synaptic output. However, if the predictions made in the preceeding paragraph are verified, the centrifugal nature of the interplexiform cell can be placed within a more fundamental pattern of retinal organization: the morphological and functional polarization of the dopaminergic amacrine (and potentially many other amacrine cell types as well (Vaney et al., '88; Dacey, '89a) into a postsynaptic dendritic tree and a presynaptic axon-like tree. The tendency for the axon-like processes of some amacrine cell types to project heavily into the outer plexiform layer then defines a dominant "interplexiform" pattern.

Synaptic organization of the dopaminergic amacrine: Is the axonal tree presynaptic and the dendritic tree postsynaptic?

The synaptic relationships of the identified dendritic and axonal components of the dopaminergic amacrine identified in the present study are not known. Previous studies of dopaminergic synapses, however, suggest the hypothesis that the axon-like tree is the major, if not sole, source of

Fig. 18. Comparison of the macaque dopaminergic amacrine with two identified amacrine cell types in the cat's retina. **A:** A monoamine-accumulating cell type identified in the cat's retina that also shows axon-like and dendritic components (Dacey, '88). By contrast with the dopaminergic amacrine, however, many of the axon-like processes arise as extensions of the distal ends of the major dendrites (small arrowheads) and the dendrites give rise to long branchlets. **B:** Dopaminergic amacrine cell in the macaque retina shows spiny, sparsely branching dendrites and a number of morphologically distinct axon like processes that arise from the proximal dendrites and soma and extend beyond the dendritic tree. **C:** The dopaminergic amacrine cell in the cat's retina. As in the macaque dopaminergic amacrine cell an axon-like process issues from the cell body and extends beyond the dendritic tree. The dendrites are long and sparsely branched and appear to show fewer spines than the macaque equivalent. By contrast with the macaque the cat dopaminergic cell tends to show only a single axon-like process originating from the cell body. This process then gives rise to a number of distinct collateral branches that bear varicosities.

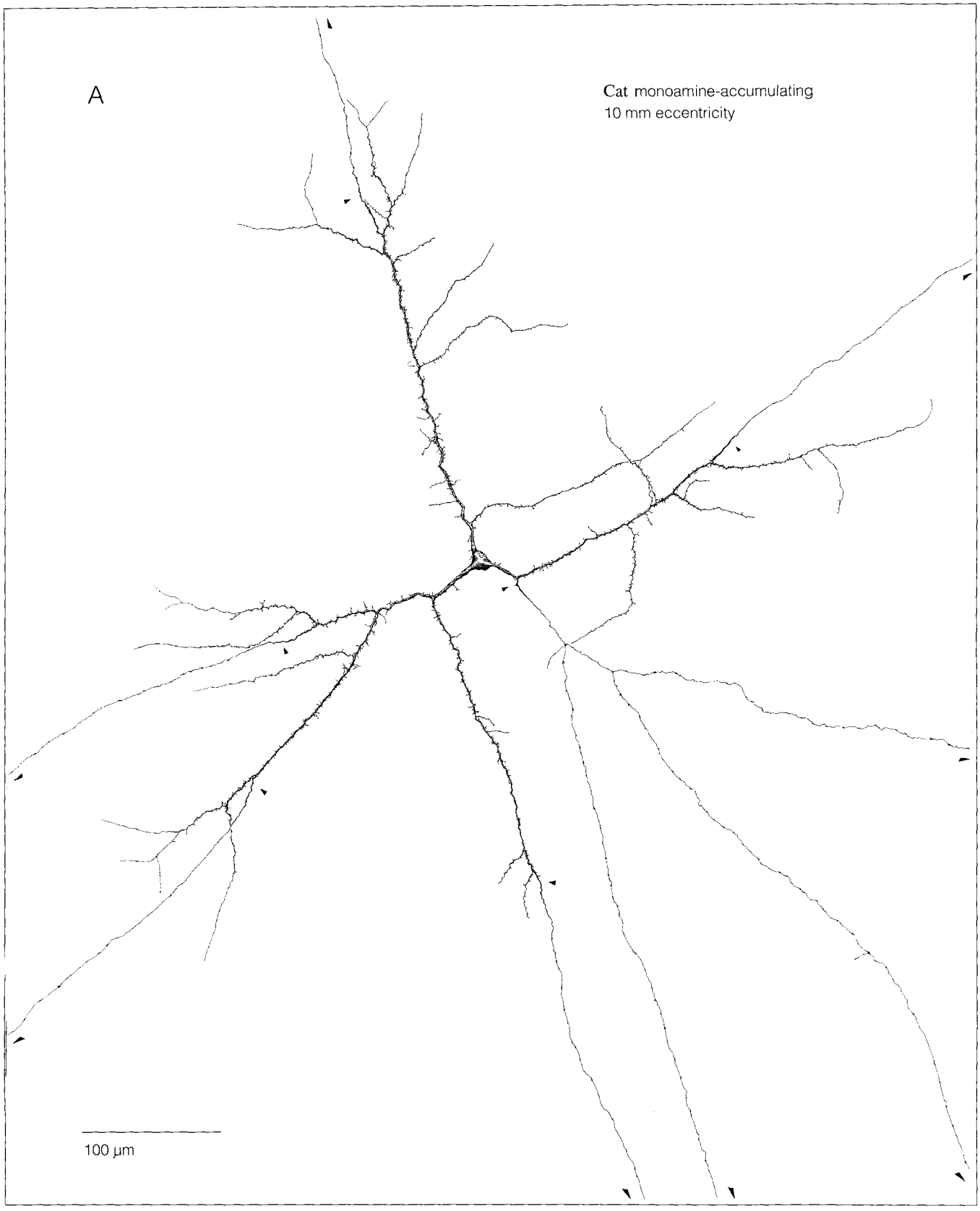

Figure 18

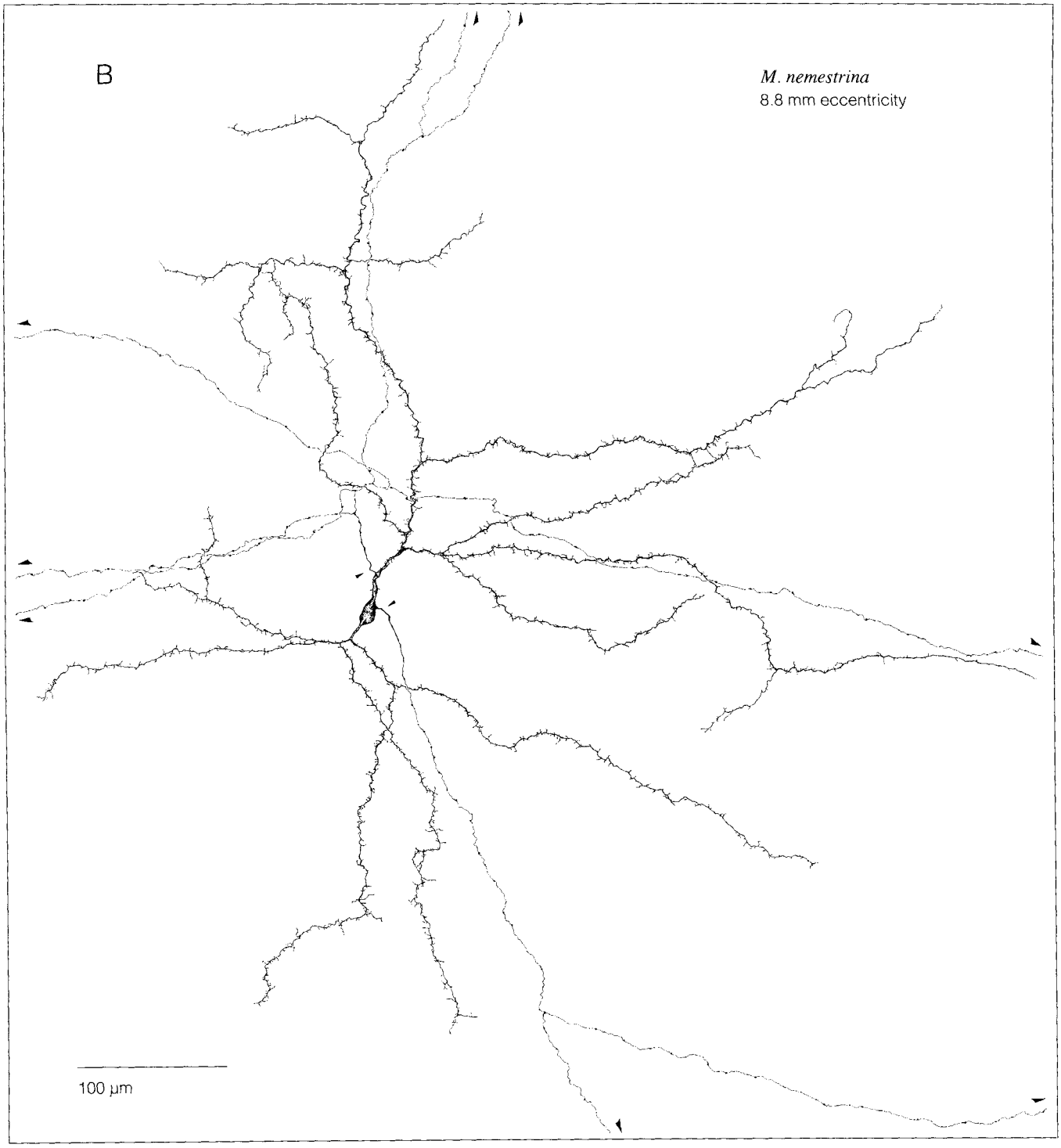

Figure 18 continued

synaptic output and the spiny, dendritic tree is the sole recipient of synaptic input. Uptake of 5,6-DHT or autoradiographic localization after [^{3}H]dopamine uptake showed the great majority of dopaminergic synapses to be presynaptic to other amacrine cell somata and dendrites (Dowling and Ehinger, '75, '78; Holmgren, '82). Two aspects of these observations were noteworthy. First, synaptic inputs to the dopaminergic amacrine were rarely observed. For example, in a study of dopaminergic synapses in *M. fascicularis*, output synapses accounted for 95% of the labeled contacts (Holmgren, '82). Second, synaptic inputs, when they were observed, were not reciprocally associated with the output synapses. Typically, synaptic output was derived from an apparent varicosity and synaptic input was restricted to

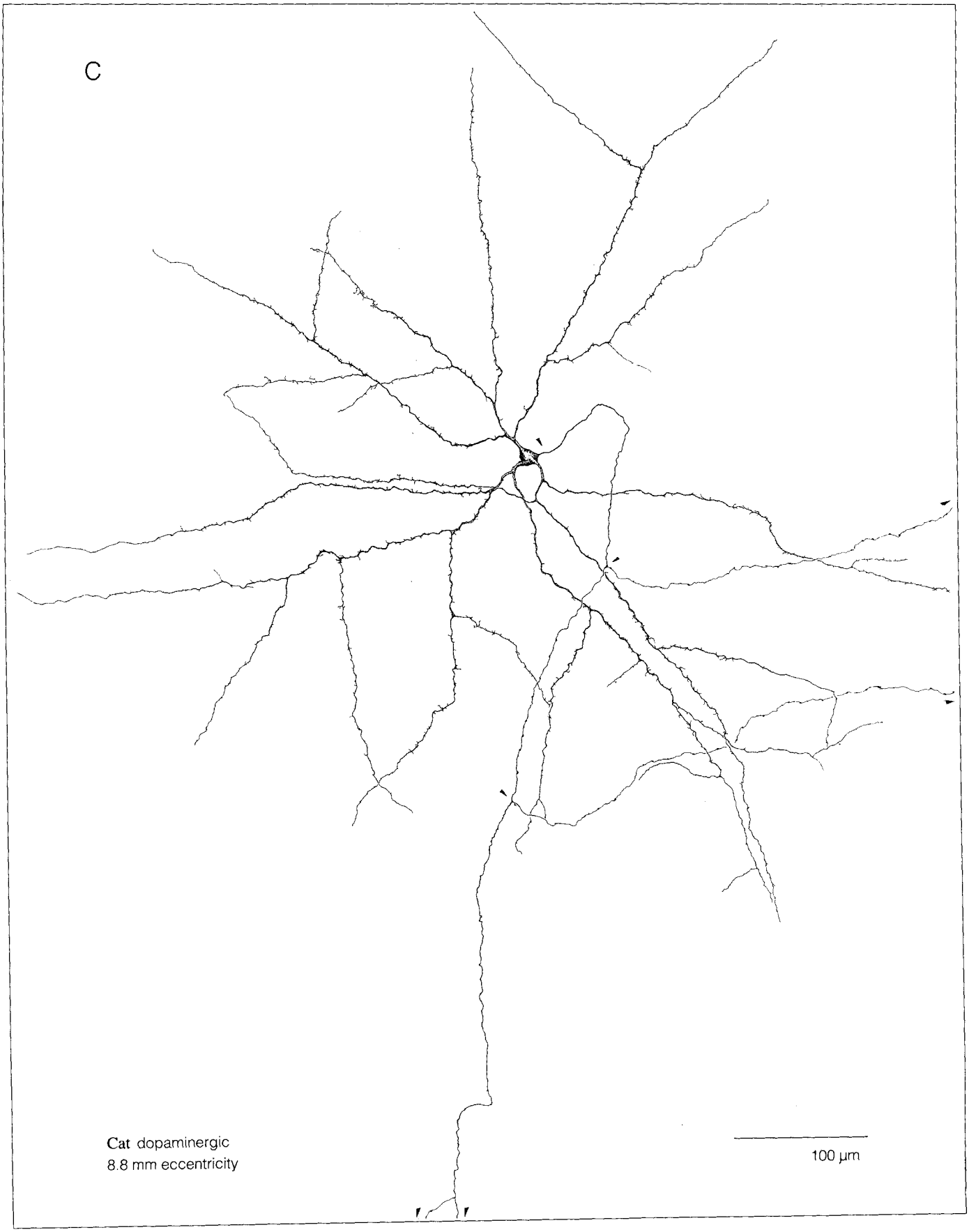

Figure 18 continued

thin dendritic or "intervaricose" segments. One conclusion drawn from these early studies was that the synaptic outputs from the dopaminergic amacrine cell far outnumbered synaptic inputs to this cell. Given that the axon-like component makes up the great mass of dopaminergic processes it is logical to hypothesize that these processes would be the predominant profile in an electron microscopic sample, and would thus be the origin of the synaptic outputs. More recent electron microscopic studies, discussed below, are consistent with this interpretation.

TABLE 1. Summary of Some of the Morphological Properties of the Large Dopaminergic Amacrine Cell Type in the Macaque Retina[1]

Morphological description	Sparsely branching, spiny dendritic tree; multiple axon-like processes bearing varicosities arise from the soma and proximal dendrites, branch sparsely and extend for mm beyond the dendritic field
Dendritic branchpoints[2]	12.6 ± 1.9, range = 9–17
Soma diameter (μm)	13.5 ± 1.1, range = 11.2–16.6
Dendritic field diameter (μm)	510 ± 82, range = 300–730
Axonal field diameter (μm)	3,000 ± 800, range = 1,000–5,400
Major depth of stratification	
Dendritic	Narrowly monostratified near outer border of IPL, rare dendrites extend to inner IPL
Axon-like processes	Narrowly monostratified near outer border of IPL, rare processes extend to INL-OPL
Spatial density[3]	10–50 cells/mm^2 (peak density ~ 0.5 mm from foveal center)
Mean coverage[4]	
Dendritic field	2.7
Axon-like field	320

[1]The label "dopaminergic amacrine cell" is used here to denote the large, intensely TH-immunoreactive amacrine cell type that shows a principal stratification near the outer border of the inner plexiform layer.
[2]All measurements are given as mean ± standard deviation.
[3]Spatial density was determined in wholemounts of TH-immunoreactive retinas. The large intensely staining cells with dendritic stratification near the outer border of the inner plexiform layer were counted. Other cell types that were less immunoreactive and showed different levels of stratification were not included in this study.
[4]Calculated by multiplying the mean spatial density of the TH-immunoreactive cells by the dendritic and axonal field areas of the HRP-filled DA-like cells described in this study. Evidence for the equivalence of the two groups of cells is given in the Results.

A major amacrine cell target of the dopaminergic synaptic output has been identified as the AII amacrine cell. The distinct ringlike clusters of varicosities observed using catecholamine histofluorescence (Mariani et al., '84; Törk and Stone, '79) or TH immunoreactivity (Brecha et al., '84; Oyster et al., '85) are the sites of dense synaptic input to the somata and proximal dendrites of this cell type (Pourcho, '82; Voigt and Wässle, '87). Dopaminergic synapses onto the somata and proximal dendrites of the AII amacrine cell do not receive reciprocal synaptic input. Given that the varicose plexus comprises the majority of TH-immunoreactive processes, it is logical to hypothesize that the varicosities on the fine processes are the source of abundant non-reciprocated synaptic outputs to the AII amacrine. The morphology of the HRP-filled cells suggests strongly that the axon-like component must be the source of the varicose plexus and therefore must be the source of the major synaptic output of the dopaminergic amacrine cells, and by the convergence of many processes create the ringlike baskets that contact the AII amacrine cell (Fig. 12E, 20).

Recent electron microscopic observations of TH immunoreactivity in cat, rabbit, and rhesus macaque retinas are consistent with, and further extend, this picture of the synaptic organization of the dopaminergic amacrine (Hokoc and Mariani, '87, '88). In the rhesus monkey, as noted previously, the great majority of synaptic contacts (80%) were presynaptic to other amacrine cells and of these virtually all (96%) were not associated with a synaptic input. An additional finding was that about half of the synaptic input was from cone bipolar cell axon terminals. These synaptic terminals as well as those of other amacrine cells virtually all (112 of 116 synapses) lacked reciprocal input from the dopaminergic process. It is reasonable to conclude that there is a physical separation between the synaptic output from the axon-like processes and the

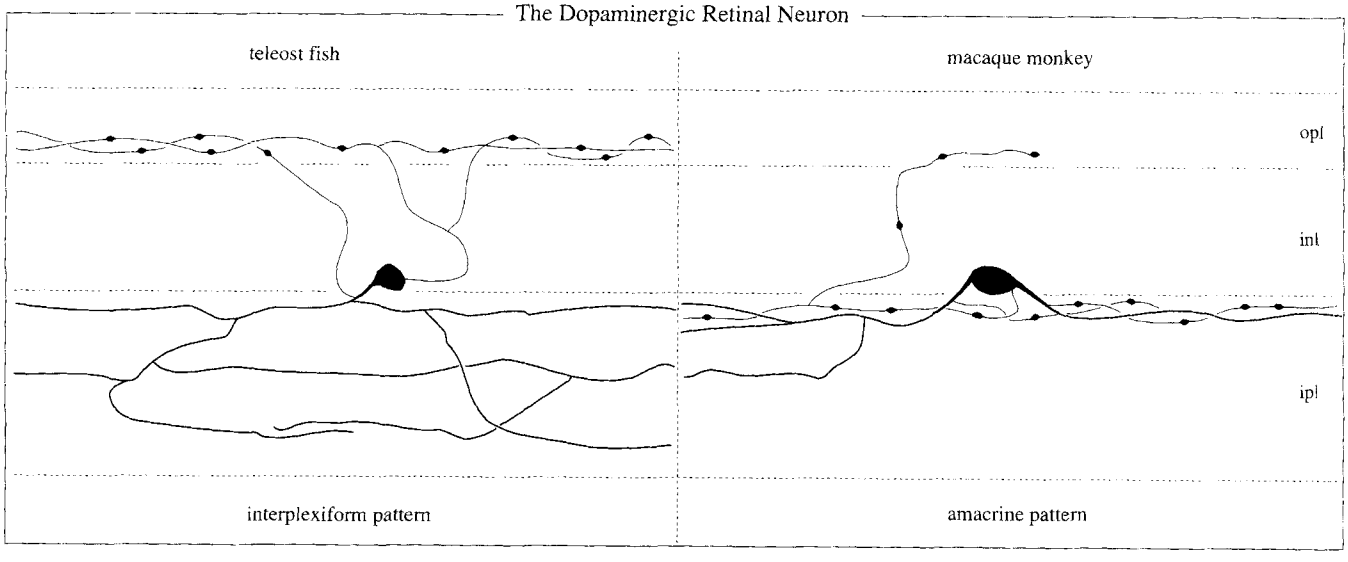

Fig. 19. Hypothesis that the dopaminergic amacrine and the dopaminergic interplexiform cell constitute a single cell type. Intracellular dye injections into carp dopaminergic interplexiform cells shows that these cells also give rise to distinct axon-like processes (Teranishi and Negishi, '88). The axon-like processes are thin and varicose and arise from the soma and proximal dendrites and extend into the outer plexiform layer. The overall pattern suggests the hypothesis that the dopaminergic amacrine cell and the dopaminergic interplexiform cell of teleost fish represent equivalent cell types that vary quantitatively across species in the degree to which the morphologically distinct axon-like processes extend into the outer retina.

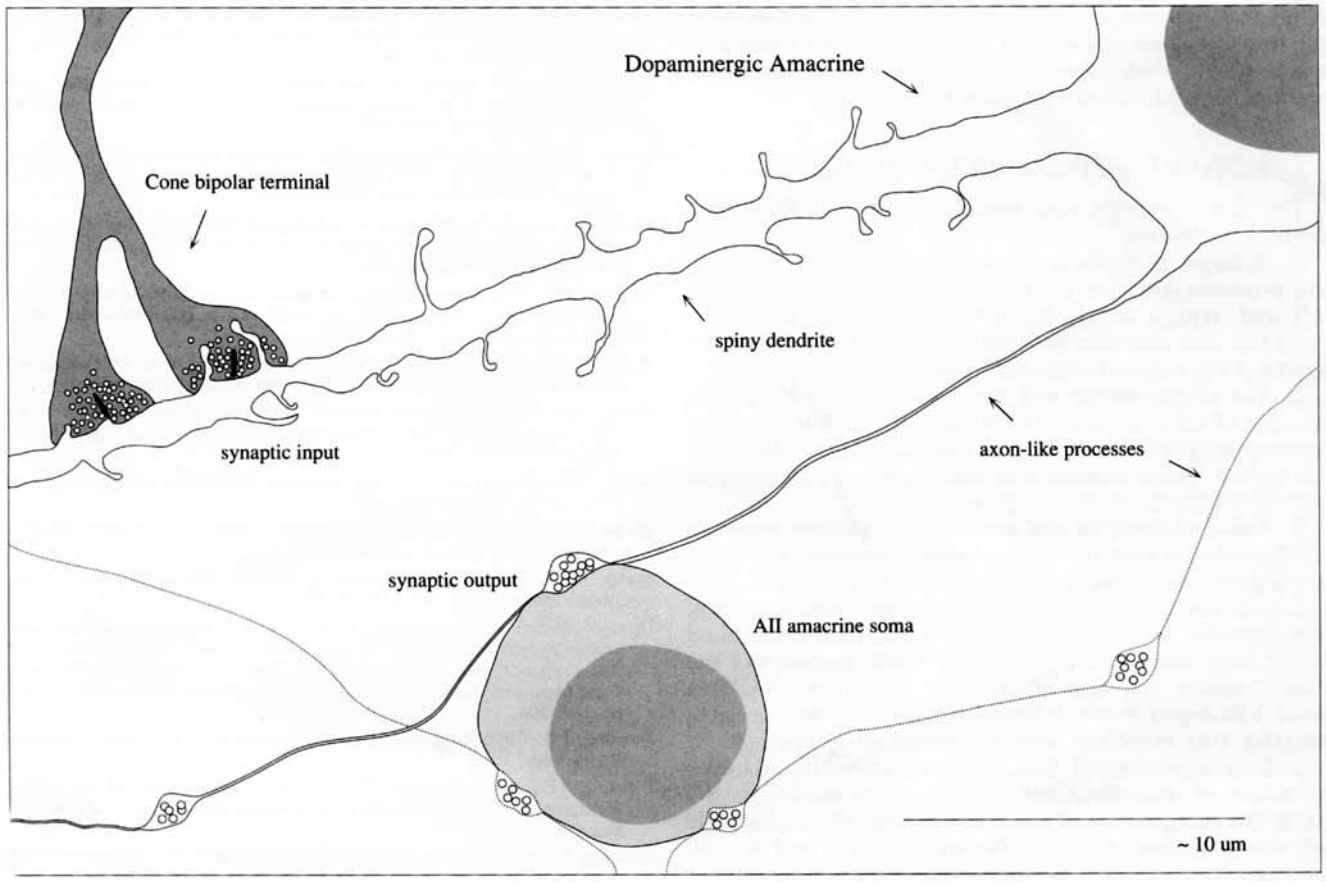

Fig. 20. Hypothesis of the synaptic organization of the dopaminergic amacrine cell. The morphology of the dopaminergic amacrine, taken together with the previous electron microscopic results considered in the Discussion, suggests the following hypothesis of synaptic organization. The varicosities along the axon-like processes account for the great majority of the synaptic output and do not receive synaptic input. The soma (and proximal dendrites) of the AII-glycine accumulating rod amacrine is one major target for the presynaptic varicosities. The dense input to the AII amacrines must arise by convergence of varicosities from a number of axon-like processes. Input from cone bipolar cells and other amacrine cell types is restricted to the spiny dendritic tree. This figure does not illustrate a second, perhaps minor source of synaptic output that may derive from the dendritic tree in the form of a morphologically distinct reciprocal synapse with the cone bipolar input.

synaptic input from cone bipolar and other amacrine cells. Either the synaptic input is restricted to the fine intervaricose segments or, as is obviously more likely, it is restricted to the thick, spiny dendritic tree of the cell.

The morphology of the dopaminergic amacrine shown in the present results, taken together with the previous EM results noted above, suggests the following hypothesis of synaptic organization (Fig. 20). The varicosities along the axon-like processes account for the great majority of the synaptic output; these boutons do not receive synaptic input. The soma (and proximal dendrites) of the AII amacrine are major targets of these presynaptic varicosities. The dense input to the AII amacrines must arise by convergence of varicosities from a number of axon-like processes. Input from cone bipolar cells and other amacrine cell types is restricted to the spiny dendritic tree. A second, apparently minor source of synaptic output may derive from the dendritic tree in the form of a morphologically distinct reciprocal synapse with the cone bipolar input.

The morphological dichotomy and the possible physical separation of synaptic input from output suggests the traditional picture of a true axon-bearing neuron and leads to the obvious question of whether these cells generate spikes that propagate along the multiple axon-like processes. This hypothesis has been discussed previously (Dacey, '88, '89a), but it is most important to note here that recent studies of transient, possibly spike generating amacrine cell types in the non-mammalian retina also suggests that these cells have both a central dendritic tree and a widely-spreading axon-like tree (Ammermuller and Weiler, '88; Djamgoz et al., '85; Teranishi et al., '87). Moreover, there is physiological evidence that the receptive fields of these cells are small and matched to dendritic field size (Ammermuller and Weiler, '88), and that the synaptic outputs of some wide field amacrine cells extend for long distances beyond a central region of synaptic input (Werblin et al., '88).

It has been noted that the dopaminergic synapse onto the AII amacrine is situated to influence the transmission of rod signals from the AII amacrine to ganglion cells. Because the AII amacrines are coupled to each other and to cone bipolar cells in the ON sublamina of the inner plexiform layer, it has also been naturally speculated in analogy with previous findings in the teleost retina (Dowling, '86) that the release of dopamine may act to electrically uncouple these gap junctions via an intracellular second messenger.

While this hypothesis remains to be tested, it is clear that the unusual geometry created by the long, axon-like processes provides an important new clue to the functional significance of the dopaminergic synapse.

CONCLUSIONS AND HYPOTHESES

The main findings and hypotheses of this study are summarized below:

1. Multiple axon-like processes originate from the soma and proximal dendrites of the large dopaminergic amacrine cell and extend widely beyond the dendritic tree. The axon-like tree accounts for a minimum of 80% of the total length of the dopaminergic cell's processes.

2. The dopaminergic cell can be distinguished from a number of other amacrine cells types that show the axon-bearing property, including a monoamine-accumulating cell type of the cat's retina that was suggested previously to correspond to the dopaminergic amacrine cell.

3. The dual dendritic and axon-like morphology suggests the hypothesis that the dopaminergic amacrine cells and the dopaminergic interplexiform cells represent equivalent cell types that show morphological variation across species. The axon-like components of the amacrine cell correspond structurally and functionally to the distal processes of the interplexiform cell that extend into the outer plexiform layer. The degree to which the axon-like component projects into the outer plexiform layer is variable across species.

4. It is hypothesized that, like the outwardly directed processes of interplexiform cells, the varicosities on the axon-like components of the dopaminergic amacrine cells are the principal source of synaptic output and do not receive synaptic input. Synaptic inputs from cone bipolar cells and other amacrine cells are restricted to the dendritic tree.

5. It is hypothesized that overlapping axon-like processes construct the varicose plexus observed in TH-immunoreacted retinas. Single processes probably extend on the order of 4 mm from their parent cell. Multiple dopaminergic synapses on the somata of AII amacrine cells must therefore arise by the convergence of axon-like processes from parent cells spread widely over the retina. Conversely, the axon-like processes arising from a single dopaminergic amacrine must diverge to make synaptic contact with a large number of AII amacrine cells.

6. Given the suggestive morphology and the great distances that may separate synaptic input from output, it is hypothesized that synaptic inputs to the dendritic tree influence the release of dopamine at distant synapses by regenerative potentials that occur near the point of origin of the axon-like process.

ACKNOWLEDGMENTS

This work was supported by NIH grant EY06678 and by NIH grant RR00166 to the Regional Primate Center at the University of Washington. I thank Bill Gardiner and Andre Lagrange for technical assistance, and Christine Curcio, Dave Marshak, Stuart Mangel, Clyde Oyster, Kate Mulligan, and Helen Sherk for reviewing drafts of this paper.

LITERATURE CITED

Ames, A., and F.B. Nesbett (1981) In vitro retina as an experimental model of the central nervous system. J. Neurochem. *37*:867–877.

Ammermuller, J., and R. Weiler (1988) Physiological and morphological characterization of OFF-center amacrine cells in the turtle retina. J. Comp. Neurol. *273*:137–148.

Brecha, N.C., C.W. Oyster, and E.S. Takahashi (1984) Identification and characterization of tyrosine hydroxylase immunoreactive amacrine cells. Invest. Ophthalmol. *25*:66–70.

Brown, K.T., and D.G. Flaming (1986) Advanced Micropipette Techniques for Cell Physiology. IBRO Handbook Series: Methods in the Neurosciences. Great Britain: John Wiley & Sons.

Buhl, E.H., and L. Peichl (1986) Morphology of rabbit retinal ganglion cells projecting to the medial terminal nucleus of the accessory optic system. J. Comp. Neurol. *253*:163–174.

Dacey, D.M. (1985) Wide-spreading terminal axons in the inner plexiform layer of the cat's retina: evidence for intrinsic axon collaterals of ganglion cells. J. Comp. Neurol. *242*:247–262.

Dacey, D.M. (1986) Distinct dendritic components of large field amacrine cells in the cat's retina. Proc. Soc. Neurosci. *12*:199 (Abstract).

Dacey, D.M. (1988) Dopamine-accumulating amacrine cells revealed by in vitro catecholamine-like fluorescence display a unique morphology. Science *240*:1196–1198.

Dacey, D.M. (1989a) Axon-bearing amacrine cells of the macaque monkey retina. J. Comp. Neurol. *284*:275–293.

Dacey, D.M. (1989b) Monoamine-accumulating ganglion cell type of the cat's retina. J. Comp. Neurol. *288*:59–80.

Dacey, D.M. (1990) The dopaminergic amacrine cell of the cat's retina. Invest. Ophthalmol. Visual Sci. *31*:535.

Djamgoz, M.B.A., J.E.G. Downing, E. Wagner, H.-J. Wagner, and I. Zeutzius (1985) Functional organization of amacrine cells in the teleost fish retina. In A. Gallego, P. Gouras (eds): Neurocircuitry of the Retina, A Cajal Memorial. Amsterdam, The Netherlands: Elsevier Publishing Co., pp. 188–204.

Dowling, J.E. (1986) Dopamine: a retinal neuromodulator? Trends Neurosci. *9*:236–240.

Dowling, J.E., and B. Ehinger (1975) Synaptic organization of the amine-containing interplexiform cells of the goldfish and Cebus monkey retina. Science. *188*:270–273.

Dowling, J.E., and B. Ehinger (1978) Synaptic organization of dopaminergic neurons in the rabbit retina. J. Comp. Neurol. *180*:203–220.

Famiglietti, E.V., and H. Kolb (1975) A bistratified amacrine cell and synaptic circuitry in the inner plexiform layer of the retina. Brain Res. *84*:293–300.

Hokoc, J.N., and A.P. Mariani (1987) Tyrosine hydroxylase immunoreactivity in the rhesus monkey retina reveals synapses from bipolar cells to dopaminergic amacrine cells. J. Neurosci. *7*:2785–2793.

Hokoc, J.N., and A.P. Mariani (1988) Synapses from bipolar cells onto dopaminergic amacrine cells in cat and rabbit retinas. Brain Res. *461*:17–26.

Holmgren, I. (1982) Synaptic organization of the dopaminergic neurons in the retina of the cynomolgus monkey. Invest. Ophthalmol. Vis. Sci. *22*:8–24.

Jensen, R.J., and N.W. Daw (1984) Effects of dopamine antagonists on receptive fields of brisk and directionally selective cells in the rabbit retina. J. Neurosci. *4*:2972–2985.

Jensen, R.J., and N.W. Daw (1986) Effects of dopamine and its agonists and antagonists on the receptive field properties of ganglion cells in the rabbit retina. Neuroscience *17*:837–855.

Mariani, A.P., and J.N. Hokoc (1988) Two types of tyrosine hydroxylase-immunoreactive amacrine cell in the rhesus monkey. J. Comp. Neurol. *276*:81–91.

Mariani, A.P., H. Kolb, and R. Nelson (1984) Dopamine-containing amacrine cells of rhesus monkey retina parallel rods in spatial distribution. Brain Res. *322*:1–7.

Negishi, K. (1981) Density of retinal catecholamine-accumulating cells in different sized goldfish. Exp. Eye Res. *33*:223–232.

Negishi, K., S. Kato, T. Teranishi, H. Kiyama, Y. Katayama, and M. Tohyama (1985) So-called interplexiform cells immunoreactive to tyrosine hydroxylase or somatostatin in rat retina. Brain Res. *346*:136–140.

Nguyen-Legros, J. (1988) Morphology and distribution of catecholamine-neurons in mammalian retina. In N.N. Osborne and G.J. Chader (eds): Progress in Retinal Research. Oxford: Pergamon Press, pp. 113–147.

Nguyen-Legros, J., B. Berger, A. Vigny, and C. Alvarez (1981) TH-like immunoreactive interplexiform cells in the rat retina. Neurosci. Lett. *27*:255–259.

Nguyen-Legros, J., C. Versaux-Botteri, L.H. Phuc, A. Vigny, and M. Gay

(1984) Morphology of primate's dopaminergic amacrine cells as revealed by TH-like immunoreactivity on retinal flatmounts. Brain Res. *295:*145–153.

Oyster, C.W., E.S. Takahashi, M. Cilluffo, and N.C. Brecha (1985) Morphology and distribution of tyrosine hydroxylase-like immunoreactive neurons in the cat retina. Proc. Natl. Acad. Sci. USA *82:*6335–6339.

Packer, O., A.E. Hendrickson, and C.A. Curcio (1990) Developmental redistribution of photoreceptors across the Macaca nemestrina (pigtail macaque) retina. J. Comp. Neurol. *298:*472–493.

Pourcho, R.G. (1982) Dopaminergic amacrine cells in the cat retina. Brain Res. *252:*101–109.

Ryan, M.K., and A.E. Hendrickson (1987) Interplexiform cells in the macaque monkey retina. Exp. Eye Res. *45:*57–66.

Savy, C., J. Yelnik, E. Martin-Martinelli, I. Karpouzas, and J. Nguyen-Legros (1989) Distribution and spatial geometry of dopamine interplexiform cells in the rat retina: I. Developing retina. J. Comp. Neurol. *289:*99–110.

Sterling, P. (1983) Microcircuitry of the cat retina. Annu. Rev. Neurosci. *6:*148–185.

Strettoi, E., E. Raviola, and R.F. Dacheux (1989) Synaptic connections of AII amacrine cells in the rabbit retina. Proc. Soc. Neurosci. *15:*968 (Abstract).

Takahashi, E. (1988) Dopaminergic neurons in the cat retina. Am. J. Optom. Physiol. Opt. *65:*331–336.

Tauchi, M., and R.H. Masland (1985) Local order among the dendrites of an amacrine cell population. J. Neurosci. *5:*2494–2501.

Tauchi, M., and R.H. Masland (1988) Morphology of the catecholaminergic neurons in the rabbit retina. Biomedical Res. *9:*135–138.

Teranishi, T., and K. Negishi (1986) Dendritic morphology of dopaminergic cells revealed by intracellular injection of Lucifer yellow in fixed carp retina. Brain Res. *370:*196–199.

Teranishi, T., and K. Negishi (1988) Regional difference in the dendritic morphology of dopamine cells in carp retina. Dev. Brain Res. *39:*9–17.

Teranishi, T., K. Negishi, and S. Kato (1987) Functional and morphological correlates of amacrine cells in carp retina. Neuroscience *20:*935–950.

Thier, P., and V. Alder (1984) Action of iontophoretically applied dopamine on cat retinal ganglion cells. Brain Res. *292:*109–121.

Törk, I., and J. Stone (1979) Morphology of catecholamine-containing amacrine cells in the cat's retina. Brain Res. *169:*261–273.

Vaney, D.I. (1985) The morphology and topographic distribution of AII amacrine cells in the cat retina. Proc. R. Soc. Lond. (Biol.) *224:*475–488.

Vaney, D.I., L. Peichl, and B.B. Boycott (1988) Neurofibrillar long range amacrine cells in mammalian retinae. Proc. R. Soc. Lond. (Biol.) *235:*203–219.

Versaux-Botteri, C., E. Martin-Martinelli, J. Nguyen-Legros, M. Geffard, A. Vigny, and L. Denoroy (1986) Regional specialization of the rat retina: catecholamine-containing amacrine cell characterization and distribution. J. Comp. Neurol. *243:*422–433.

Voigt, T., and H. Wässle (1987) Dopaminergic innervation of AII amacrine cells in the mammalian retina. J. Neurosci. *12:*4115–4128.

Wässle, H., B.B. Boycott, and R.B. Illing (1981) Morphology and mosaic of on- and off-beta cells in the cat retina and some functional considerations. Proc. R. Soc. Lond. (Biol.) *212:*177–195.

Wässle, H., and M.H. Chun (1988) Dopaminergic and indoleamine-accumulating amacrine cells express GABA-like immunoreactivity in the cat retina. J. Neurosci. *8:*3383–3394.

Wässle, H., L. Peichl, and B.B. Boycott (1981) Morphology and topography of on- and off-alpha cells in the cat retina. Proc. R. Soc. Lond. (Biol.) *212:*157–175.

Werblin, F., G. Maguire, P. Lukasiewicz, S. Eliasof, and S.M. Wu (1988) Neural interactions mediating the detection of motion in the retina of the tiger salamander. Vis. Neurosci. *1:*317–329.